Europ. J. Agronomy 82 (2017) 144–162

Contents lists available at ScienceDirect

European Journal of Agronomy

journal homepage: www.elsevier.com/locate/eja

Designing future barley ideotypes using a crop model ensemble

Fulu Tao[a,*], Reimund P. Rötter[a,b], Taru Palosuo[a], C.G.H. Díaz-Ambrona[c], M. Inés Mínguez[c], Mikhail A. Semenov[d], Kurt Christian Kersebaum[e], Claas Nendel[e], Davide Cammarano[f], Holger Hoffmann[g], Frank Ewert[g], Anaelle Dambreville[h], Pierre Martre[h], Lucía Rodríguez[c], Margarita Ruiz-Ramos[c], Thomas Gaiser[g], Jukka G. Höhn[a], Tapio Salo[a], Roberto Ferrise[i], Marco Bindi[i], Alan H. Schulman[a,j]

[a] Natural Resources Institute Finland (Luke), FI-00790 Helsinki, Finland
[b] Department of Crop Sciences, Georg-August-University Göttingen, Grisebachstr. 6, 37077 Göttingen, Germany
[c] AgSystems–CEIGRAM Research Centre for Agricultural and Environmental Risk Management-Technical University of Madrid, Spain
[d] Computational and Systems Biology Department, Rothamsted Research, Harpenden, Herts AL5 2JQ, UK
[e] Institute of Landscape Systems Analysis, Leibniz Centre for Agricultural Landscape Research, 15374 Müncheberg, Germany
[f] The James Hutton Institute, Invergowrie, Dundee, DD2 5DA Scotland, UK
[g] Crop Science Group, INRES, University of Bonn, Katzenburgweg 5, 53115 Bonn, Germany
[h] UMR LEPSE, INRA, Montpellier SupAgro, 34 060 Montpellier, France
[i] Department of Agri-Food Production and Environmental Sciences—University of Florence, Piazzale delle Cascine 18, 50144 Firenze, Italy
[j] Institute of Biotechnology, University of Helsinki, FIN-00014 Helsinki, Finland

ARTICLE INFO

Article history:
Received 4 July 2016
Received in revised form 20 October 2016
Accepted 22 October 2016
Available online 6 November 2016

Keywords:
Adaptation
Breeding
Climate change
Crop simulation models
Impact
Genotype
Genetic traits

ABSTRACT

Climate change and its associated higher frequency and severity of adverse weather events require genotypic adaptation. Process-based ecophysiological modelling offers a powerful means to better target and accelerate development of new crop cultivars. Barley (*Hordeum vulgare* L.) is an important crop throughout the world, and a good model for study of the genetics of stress adaptation because many quantitative trait loci and candidate genes for biotic and abiotic stress tolerance have been identified in it. Here, we developed a new approach to design future crop ideotypes using an ensemble of eight barley simulation models (i.e. APSIM, CropSyst, HERMES, MCWLA, MONICA, SIMPLACE, *SiriusQuality*, and WOFOST), and applied it to design climate-resilient barley ideotypes for Boreal and Mediterranean climatic zones in Europe. The results showed that specific barley genotypes, represented by sets of cultivar parameters in the crop models, could be promising under future climate change conditions, resulting in increased yields and low inter-annual yield variability. In contrast, other genotypes could result in substantial yield declines. The most favorable climate-zone-specific barley ideotypes were further proposed, having combinations of several key genetic traits in terms of phenology, leaf growth, photosynthesis, drought tolerance, and grain formation. For both Boreal and Mediterranean climatic zones, barley ideotypes under future climatic conditions should have a longer reproductive growing period, lower leaf senescence rate, larger radiation use efficiency or maximum assimilation rate, and higher drought tolerance. Such characteristics can produce substantial positive impacts on yields under contrasting conditions. Moreover, barley ideotypes should have a low photoperiod and high vernalization sensitivity for the Boreal climatic zone; for the Mediterranean, in contrast, it should have a low photoperiod and low vernalization sensitivity. The drought-tolerance trait is more beneficial for the Mediterranean than for the Boreal climatic zone. Our study demonstrates a sound approach to design future barley ideotypes based on an ensemble of well-tested, diverse crop models and on integration of knowledge from multiple disciplines. The robustness of model-aided ideotypes design can be further enhanced by continuously improving crop models and enhancing information exchange between modellers, agro-meteorologists, geneticists, physiologists, and plant breeders.

1. Introduction

The global demand for agricultural crop production is expected to roughly double by 2050 according to the projected increases

---

* Corresponding author.
E-mail address: fulu.tao@luke.fi (F. Tao).

http://dx.doi.org/10.1016/j.eja.2016.10.012
1161-0301/

in population (Gerland et al., 2014), consumption, and changes in diets (Godfray et al., 2010; Tilman et al., 2011). However, climate change and weather extremes will exacerbate the constraints on increasing food supplies and food security (Ray et al., 2015). Recently, the IPCC (Porter et al., 2014) reported that for the major crops (wheat, rice, and maize) in tropical and temperate regions, without adaptation, climate change will have negative impacts on production when local temperature increases by 2 °C or more above late-20th-century levels, although it also may have positive impacts at some individual locations. Furthermore, some studies suggest that climate change may progressively increase the inter-annual variability of crop yields in some regions, resulting in an increased risk of more severe impacts (Porter et al., 2014; Ray et al., 2015). In recent years, yields for important crops have stagnated in several important agricultural regions around the world due to changes in climate and agronomic management (Peltonen-Sainio et al., 2008; Brisson et al., 2010; Ray et al., 2012; Grassini et al., 2013; Tao et al., 2015), although in some other parts of the world yields have kept increasing despite ongoing climate change as a consequence of new cultivars and improved crop management (Ray et al., 2012; Tao et al., 2012, 2015).

Crop cultivar development and improved agronomic practices are pivotal to climate change adaptation for agriculture (Hatfield et al., 2011; Tao et al., 2012; Challinor et al., 2014; Ewert et al., 2015; Rötter et al., 2015). One of the most effective adaptation options for future climates is the development of climate resilient crop cultivars (Tao and Zhang, 2010; Challinor et al., 2014). In parallel, agronomists are trying to develop new agronomic practices for a changing climate (FAO, 2010). Plant breeders are increasingly using genomics and biotechnology to develop cultivars that have greater yield stability (lower inter-annual yield variation) in our current production systems (Mir et al., 2012). It is, however, difficult to develop crop ideotypic traits for a targeted environment (Reynolds et al., 2016). It is also expensive in terms of labor, time, and funding requirements to determine the values of the different traits particularly under future climatic conditions (Li et al., 2012; Gouache et al., 2016).

Process-based crop models developed for simulating interactions between genotype, environment, and management are widely applied to assess impacts of environmental change on crop development, growth, and yield (Boote et al., 2001; Asseng et al., 2015), as well as to design adaptation strategies to cope with climate risk (Bergez et al., 2010; Tao and Zhang, 2010; Rötter et al., 2011a; Dumont et al., 2015). In recent decades, crop modelling has become an important tool for evaluating new cultivars (Marcaida et al., 2014; Gouache et al., 2016) and supporting plant breeding (Boote et al., 2001; Li et al., 2012; Rötter et al., 2015), in particular in the design of ideotypes, i.e. ‘model plants’, for different crops and cultivation environments (Dingkuhn et al., 1991, 2015; Martre et al., 2015a; Rötter et al., 2015; Semenov and Stratonovitch, 2013). So far, such studies are limited to individual models, which differ in terms of the number of parameters and processes and their descriptions, complexity, and functionality (Palosuo et al., 2011; Asseng et al., 2013). Drawing conclusions based on a single crop model can generate quite large biases (Asseng et al., 2013). Recently, ensemble modelling has been proposed as a valuable approach for assessing and reducing uncertainties in crop simulations (Rötter et al., 2011b; Wallach et al., 2016). The strengths of inter-model comparison and ensemble modelling have been demonstrated in many studies (e.g., Palosuo et al., 2011; Rötter et al., 2012; Asseng et al., 2013, 2015; Bassu et al., 2014; Li et al., 2015; Martre et al., 2015b).

Food supply and food security in Europe as well as in many other parts of the world especially depend on the Triticeae crops, which include wheat, barley, rye, and fodder crops. Barley (*Hordeum vulgare* L.) is a good model for study of the genetics of stress adaptation (Moshelion et al., 2015). In this study, we aim to: 1) develop a new approach to design future crop ideotypes using a crop model ensemble; 2) apply this approach to design climate-resilient barley ideotypes for Boreal and Mediterranean climatic zones in Europe, representing contrasting climatic conditions for barley production in Europe.

2. Materials and methods

2.1. Study sites

Two study sites with contrasting climates were chosen to represent the North and South of current agro-climatic conditions for barley cultivation areas in Europe. One is Jokioinen (60.81°N, 23.50°E, 104 m a.s.l.) in Finland in northern Europe, and the other is Lleida (41.63°N, 0.60°E, 190 m a.s.l.) in Spain in southern Europe (Fig. 1). Jokioinen has a Boreal climate, with an average annual mean temperature and total precipitation of 4.6 °C and 628.2 mm, respectively, over 1980–2010. Lleida has a Mediterranean climate, with an annual mean temperature and total precipitation of 15.0 °C and 340.6 mm, respectively, over 1980–2010. At Jokioinen, spring barley is generally sown in the middle of May and harvested at the end of August. At Lleida, winter barley is generally sown in the middle of November and harvested at the beginning of July. During 1980–2010, the mean temperature, precipitation, solar radiation, and photoperiod for the barley growing season was respectively 13.6 °C, 252.4 mm, 17.5 MJ m^{-2} day^{-1}, and 17.6 h at Jokioinen and 11.5 °C, 227.3 mm, 13.6 MJ m^{-2} day^{-1}, and 11.8 h at Lleida.

2.2. Data

Detailed experimental field data including soils, tillage, fertilization, phenology, yield, and biomass were obtained for two growing seasons at Jokioinen in 2002 and 2009 (Salo et al., 2016) and for three growing seasons at Lleida from 1996 to 1999 (Cantero-Martinez et al., 2003). The barley cultivars used are representative of those currently grown at each location: Annabell at Jokioinen and Hispanic at Lleida. Annabell is a modern (released after 1985) and considered late-maturing. Hispanic is a member of the Spanish barley core collection. Hispanic has a much larger thermal requirement than does Annabell. The soils were a Vertic Cambisol (IUSS, 2006) with a clay texture at Jokioinen, and Typic Xerofluvent (USDA, 1999) with a loam texture at Lleida. The experimental data used for crop model calibration and validation are summarized in Table S1.

The observed daily weather data for solar radiation, minimum and maximum temperature, precipitation, wind speed, and air humidity for 1980–2010 at the two sites were obtained from the Finnish Meteorological Institute, the Spanish Agencia Estatal de Meteorología (AEMET), and from other sources, as detailed in Pirttioja et al. (2015).

For future climate scenarios, three representative climate projections (relatively hot, medium, and relatively cold) for the period of the 2050s, made by three global circulation models (GCMs), were selected from the Coupled Model Inter-comparison Project Phase 5 (CMIP5) ensemble, driven by the emission scenario of Representative Concentration Pathway (RCP) 8.5. The atmospheric CO_2 concentrations assumed were 360 ppm for 1980–2010 and 560 ppm for the 2050s. The three GCMs were the Hadley Centre Global Environmental Model–Earth System, version 2 (HadGEM2-ES; hereafter HadGEM) (Jones et al., 2011), the National Aeronautics and Space Administration (NASA) Goddard Institute for Space Sciences (GISS) coupled general circulation model (hereafter GISS) (Nazarenko et al., 2015), and the Australian Community Climate and Earth System Simulator (hereafter ACCESS) (Rashid et al., 2013). The climate projections were further down-scaled for local impact assessments using the LARS-WG weather generator, as

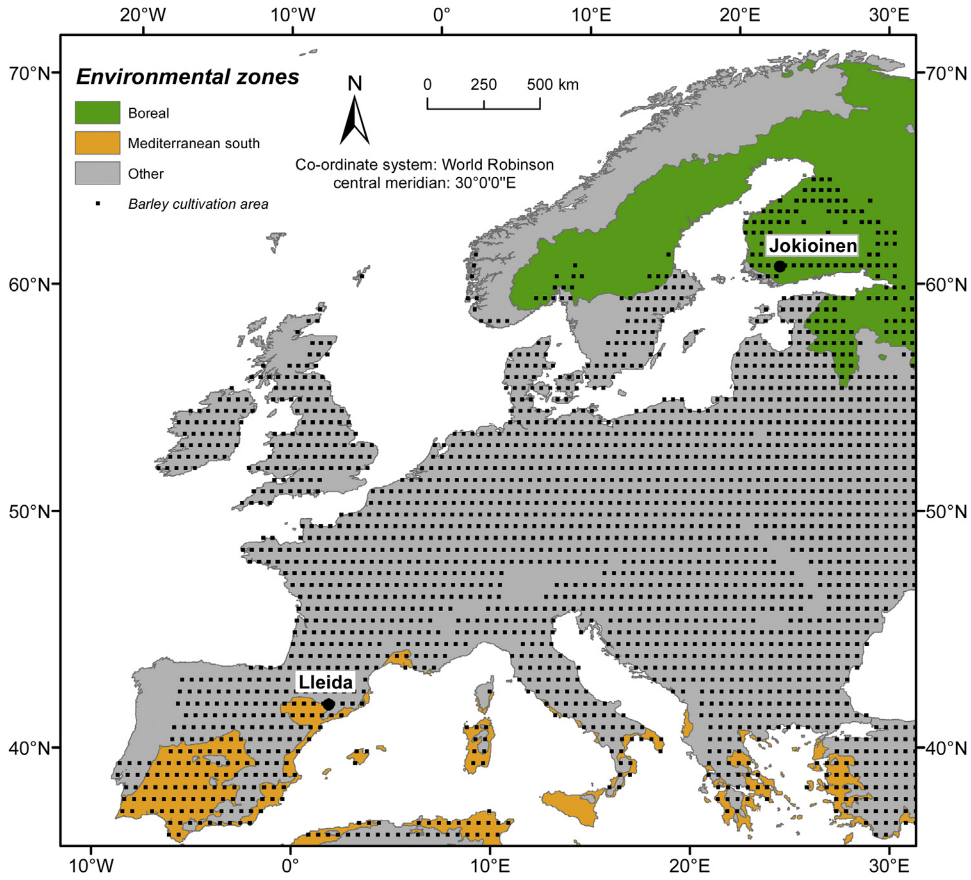

Fig. 1. Locations of experiment stations used in this study superimposed on environmental zones as defined by Metzger et al. (2005). Black squares are barley cultivation areas from Monfreda et al. (2008), re-sampled to 0.5°.

described by Semenov and Stratonovitch (2015). In this method, baseline climate statistical parameters as derived for, and incorporated into, LARS were adjusted to fit the projected climate under different scenarios. These parameters were then used in LARS-WG to generate local-scale daily climate scenario data for the future period (Semenov and Stratonovitch, 2015). Finally, daily weather data of 31 sample years representing 2050s conditions were used for crop model simulations. The simulations were further compared with simulations using the baseline climate conditions for 1980–2010.

2.3. Modelling protocol

In this study, an ensemble of eight crop models, respectively APSIM 7.7 (Keating et al., 2003), CropSyst 4.15.04 (Stöckle et al., 2003), HERMES 4.26 (Kersebaum, 2007), MCWLA 2.0 (Tao and Zhang, 2013), MONICA 1.2.5 (Nendel et al., 2011), SIMPLACE<Lintul2, Slim> (Addiscott and Whitmore, 1991), *SiriusQuality* 2.0 (Martre et al., 2006), and WOFOST 7.1 (Boogaard et al., 1998), representing different degrees of complexity and different strengths, was used for identifying future barley ideotypes. The information on the eight crop models is presented in Table S2. The approaches applied in the various crop models were summarized in Asseng et al. (2013, 2015) and Pirttioja et al. (2015). All models are dynamic and work on a daily time step. Differences among models in simulating major processes of crop development, growth, light utilization, biomass accumulation, and grain formation are briefly described below.

- Crop development: APSIM, CropSyst, HERMES, and MONICA account for temperature, photoperiod, vernalization, and other water or nutrient stress effects on phenology. MCWLA, SIMPLACE and *SiriusQuality* account for temperature, photoperiod, and vernalization. WOFOST accounts for temperature and photoperiod. *SiriusQuality* uses daily canopy mean temperature; all other models use daily air mean temperature.
- Leaf growth: APSIM, CropSyst, MCWLA, and SIMPLACE adopt a simple approach, such as leaf area index (LAI). *SiriusQuality*, HERMES, MONICA, and WOFOST adopt a detailed approach, e.g., one or more canopy layers, to simulate leaf growth.
- Drought and heat stress: for simulating drought stress, APSIM, CropSyst, MCWLA, and SIMPLACE adopt the actual to the potential evapotranspiration ratio, whereas *SiriusQuality* adopts soil-available water in the root zone. In applying the first approach, APSIM, CropSyst, MCWLA, and SIMPLACE adopt Priestley-Taylor, Penman-Monteith, Penman-Monteith, and a modified Penman approach to potential evapotranspiration, respectively. HERMES, MONICA, and WOFOST adopt a combination of both drought stress approaches. APSIM, HERMES, SIMPLACE, and WOFOST do not yet account for specific heat stress during certain phenological phases. CropSyst and MONICA account for heat stress on reproductive organs. APSIM and *SiriusQuality* account for heat stress on leaf senescence. MCWLA accounts for heat stress on both vegetative and reproductive organs.
- Light utilization and biomass accumulation: APSIM, CropSyst, *SiriusQuality*, and SIMPLACE adopt radiation use efficiency (RUE) or transpiration efficiency (TE) biomass growth approaches to simu-

late light utilization, photosynthesis, and biomass accumulation. HERMES, MCWLA, MONICA, and WOFOST adopt an approach of gross photosynthesis minus respiration.

- Grain formation: CropSyst and MCWLA adopt a harvest index (HI) approach to simulate grain formation. APSIM, HERMES, MONICA, *SiriusQuality*, SIMPLACE, and WOFOST adopt assimilate partitioning patterns to different organs to simulate grain formation; APSIM and *SiriusQuality* also account for grain number and grain weight.

Each crop model was first calibrated and validated using the detailed field experimental data for Jokioinen and Lleida (Table S1). This was done by comparing the simulated flowering date, maturity date, and yield from each crop modelling group with the corresponding observed ones. Because the crop models are process-based, we assumed that the models calibrated and validated under baseline climate conditions can be applied also under future climate conditions. For each crop model, the most important seven to eight cultivar parameters that are closely related to crop growth, development, and grain formation were identified for each crop modelling group (Table S2). Then, considering future barley cultivars, the potential value range conceivable in the future for each of the important parameters was determined by consulting experts, as well as the literature, information, knowledge and experiences that each modelling group obtained (Table S3). Next, an orthogonal sampling approach (Iman et al., 1981) was used to conduct cultivar parameter perturbations to ensure good representation of parameter variability. For each of the most important seven or eight cultivar parameters in a crop model, three representative values (V_1, V_2, V_3) across the range of the parameter values (from $V_{\min}$ to $V_{\max}$), i.e., the value at the one-sixth point ($V_1 = V_{\min} + (V_{\max} - V_{\min}) \times 1/6$), middle point ($V_2 = (V_{\min} + V_{\max})/2$), and five-sixth point ($V_3 = V_{\min} + (V_{\max} - V_{\min}) \times 5/6$), were selected. The three representative values for each of the seven to eight cultivar parameters were randomly combined, resulting in 3^n (where n is the number of the selected cultivar parameters for a crop model) sets of cultivar parameters for each crop model. Finally, with each crop model, simulations were conducted for 30 years under the baseline climate (1981–2010) and the three different projected climates for the 2050s, using the single set of calibrated parameters and 3^n sets of perturbed parameters, for Jokioinen and Lleida respectively. Current typical sowing dates were used for the simulations under both baseline and future climates. Different sowing dates may affect simulated final yields to some extent, but if well fitted to the environment, they were assumed not to affect the relative advantages of cultivar traits that we focused on in this study.

2.4. Analyses

For each crop model, the simulated yield changes between the three different projected climates for the 2050s and the baseline climate (1981–2010), using the single set of calibrated parameters and the 3^n sets of perturbed parameters, were first analyzed and compared. Then, based on the simulated changes in mean yield and yield variability across the three different climate scenarios for 2050s for each crop model, the simulations with the 3^n sets of perturbed cultivar parameters under the three future climate scenarios were classified into three groups. For each crop model, the high-yielding group included simulations by the 100 sets of perturbed cultivar parameters that produced the highest mean yield and lowest yield variability for the 2050s across the three different climate scenarios. The low-yielding group included the simulations by the 100 sets of perturbed cultivar parameters that produced the lowest mean yield and higher yield variability for the 2050s across the three selected climate scenarios. The simulations using the remaining (3^n-100-100) sets of perturbed parameters were classified into the middle-yielding group. Next, the corresponding model parameter sets for the simulations in the high-yielding group were further investigated to identify the desirable cultivar traits. Finally, the design of the future barley ideotypes was further refined by comparing the results from all the crop models and by combining the desirable cultivar traits respectively for Jokioinen and Lleida.

3. Results

3.1. Future climate change scenarios at the two study sites

During the 2050s, under the ACCESS, GISS, and HADGEM climate change scenarios for Jokioinen, annual mean $T_{\min}$ and $T_{\max}$ are projected to increase by 2.55 and 2.55 °C, 3.16 and 2.88 °C, and 3.60 and 3.45 °C, respectively, relative to baseline (1981–2010) climate conditions (Fig. 2). Annual total precipitation is projected to increase by 12.6 %, 6.0%, and 8.0%, respectively (Fig. 2). Annual mean solar radiation is projected to change by 4.3%, −3.5%, and 2.1%, respectively (Fig. 2). During the barley growing season, seasonal mean $T_{\min}$ and $T_{\max}$ are projected to increase by 2.60 and 2.60 °C, 2.53 and 2.44 °C, and 3.42 and 3.41 °C, respectively, relative to baseline (1981–2010) climate conditions. Seasonal mean precipitation is projected to increase by 12.5%, 5.5 %, and 2.0%, respectively. Seasonal mean solar radiation is projected to change by 2.75%, −1.5%, and 3.75%, respectively.

During the 2050s, under the ACCESS, GISS and HADGEM climate change scenarios for Lleida, annual mean $T_{\min}$ and $T_{\max}$ are projected to increase by 2.94 and 2.94 °C, 1.43 and 1.39 °C, and 2.51 and 3.28 °C, respectively, relative to baseline climate conditions (Fig. 2). Annual total precipitation is projected to change by −10.0%, 5.0%, and −10.3%, respectively (Fig. 2). Annual mean solar radiation is projected to change by 5.3%, −0.7%, and 5.5%, respectively (Fig. 2). During the barley growing season, the seasonal mean $T_{\min}$ and $T_{\max}$ are projected to increase by 2.64 and 2.64 °C, 1.30 and 1.27 °C, and 2.12 and 2.72 °C, respectively, relative to baseline (1981–2010) climate conditions. The seasonal mean precipitation is projected to decrease by 18.3%, 0.6%, and 0.9%, respectively. Seasonal mean solar radiation is projected to change by 6.0%, −1.0% and 5.3%, respectively. Summarizing, hotter and wetter climatic conditions compared to baseline were projected by ACCESS, GISS and HADGEM for Jokioinen; for Lleida, hotter and drier climatic conditions were projected. Precipitation projections for Lleida show higher uncertainty than for Jokioinen.

3.2. Calibration of crop model cultivar parameters and the parameter value ranges

For each crop model, one set of optimal parameters was calibrated and validated with the experimental field data. At both sites, the differences between simulated and observed flowering and maturity dates were less than five days, and the discrepancies between observed and simulated yield were less than 20%. The key cultivar parameters in each of the eight crop models and their calibrated values under the baseline climate for Jokioinen and Lleida are listed in Table S3. There were some differences between cultivar traits at Jokioinen and Lleida. For example, the required thermal times (in degree-days) to flowering and maturity were much larger and HI was smaller for the cultivar at Lleida (Table S3). The parameter value range identified based on literature and experts' knowledge is listed in Table S3. For each site, the value range for each parameter covered its calibrated value under baseline conditions, which suggested the parameter value could

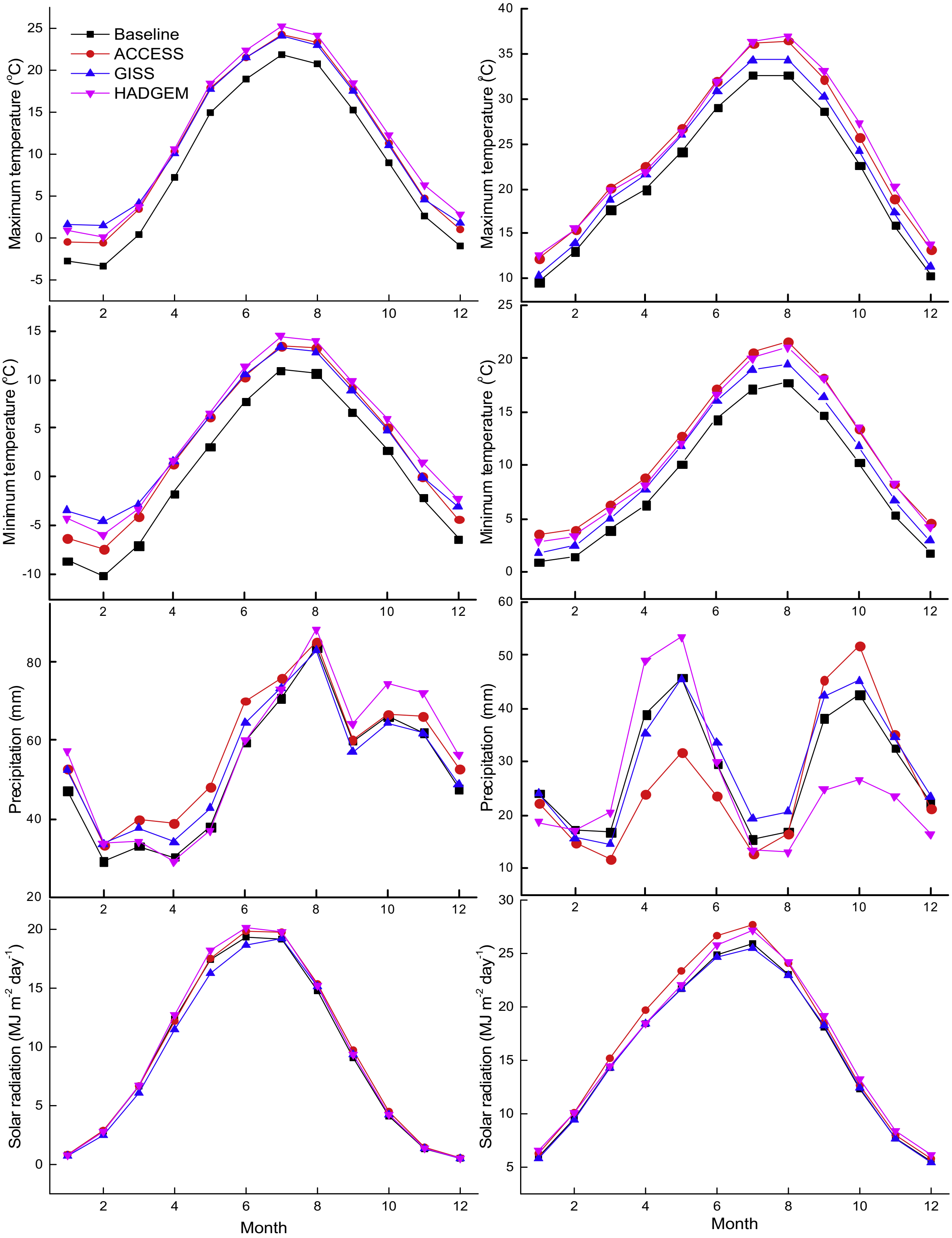

Fig. 2. Monthly mean maximum temperature, minimum temperature, precipitation and solar radiation in Jokioinen, Finland (left) and Lleida, Spain (right) during 1980–2010 and 2050s under ACCESS, GISS and HADGEM climate change scenarios.

potentially be larger or smaller than its calibrated value for the 2050s, yet still remain within a range of realistic (plausible) values.

3.3. Overall yield projections for the selected future climate scenarios

The simulated yield changes with the single set of calibrated cultivar parameters and with the 3^n sets of perturbed cultivar parameters under the three future climate scenarios are presented in Fig. 3 for Jokioinen and in Fig. 4 for Lleida, relative to the simulations under the baseline climate with the single set of calibrated cultivar parameters. The simulated yield changes varied widely among the crop models, as well as under different future climate scenarios (Figs. 3 and 4). In general, the simulated yield changes varied more among the crop models than among different future climate scenarios. Among the three future climate scenarios, barley production would be more vulnerable under the hotter HADGEM climate scenarios for Jokioinen (Fig. 3) and under the hotter and drier ACCESS climate scenarios for Lleida (Fig. 4). The results were generally consistent among the simulations by different crop models. With the single set of calibrated cultivar parameters, yield was projected to decrease under one or more future climate scenarios by APSIM, CropSyst, HERMES, SIMPLACE, and WOFOST for Jokioinen (Fig. 3) and APSIM, CropSyst, SIMPLACE, and WOFOST for Lleida (Fig. 4). This suggests that barley yield could decrease in the 2050s with current cultivars and crop management at both locations. By contrast, in the simulations with the 3^n sets of perturbed cultivar parameters, for each crop model and under each future climate scenario, some sets of cultivar parameters gave substantial yield increases at both Jokioinen (Fig. 3) and Lleida (Fig. 4). The traits of these yield-increasing cultivars (represented by their cultivar parameters) potentially can be used by breeders to develop novel climate-resilient cultivars for future climate scenarios (see, also Section 4.1).

3.4. Yield changes for high and low yielding genotypes

There were quite large differences among the simulated yield changes by different crop models, as well as under different future-climate scenarios. Yet, for the individual crop models, the simulated yield changes by the 100 sets of perturbed cultivar parameters in the high yielding group were mostly positive under the three future climate scenarios for the 2050s, relative to baseline climate conditions (except for the majority of CropSyst simulation runs). This applied at both Jokioinen (Fig. 5) and Lleida (Fig. 6). Under different future-climate scenarios, based on the simulations for the high-yielding group, barley yield was projected to change at Jokioinen on average by 5.8–18.4% for APSIM, −26.7 to 4.3% for CropSyst, 48.6–59.3% for HERMES, 55.1–70.3% for MCWLA, 61.2–76.0% for MONICA, 12.4–16.7% for SIMPLACE, 6.1–23.5% for *SiriusQuality*, and 15.7–25.5% for WOFOST (Fig. 5). The corresponding values at Lleida were 45.2–55.1% for APSIM, −40.3 to −19.0% for CropSyst, 130.4–148.9% for HERMES, 78.2–125.0% for MCWLA, 159.0–188.3% for MONICA, 25.6–52.0% for SIMPLACE, 88.7–94.6% for *SiriusQuality*, and −20.5 to 24.0% for WOFOST (Fig. 6). In contrast, simulated yield changes for the low-yielding group were negative for most of the cases at both Jokioinen (Fig. 5) and Lleida (Fig. 6). These results suggest that the new genotypes in the high-yielding group (represented by sets of genotypic parameters in crop models) could make a large difference in the effort to adapt barley production to future climates.

3.5. Identifying barley ideotypic traits under future climate scenarios

For each crop model, the values of cultivar parameters for the high-yielding group were further examined and compared to those for the middle- and low-yielding groups at Jokioinen (Table 1) and Lleida (Table 2) respectively. This was done in order to identify key traits that can be combined for designing resilient barley ideotypes under future climate conditions. With the APSIM model, at Jokioinen, the genotypic traits of the high yielding group genotypes were characterized by larger vernalization sensitivity, RUE and number of grains per gram of stem (Table 1). At Lleida, the genotypic traits of the high yielding group genotypes were characterized by larger phyllochron, RUE, CO_2 fertilization effect, grain size and number of grains per gram of stem, but smaller photoperiod and vernalization sensitivity (Table 2). With the CropSyst model, both at Jokioinen and Lleida, the genotypic traits of the high-yielding group genotypes were characterized by larger thermal time from sowing to maturity, RUE, transpiration efficiency, maximum water uptake, and harvest index (HI), but smaller thermal time from sowing to flowering, maximum LAI (LAI_{max}), and threshold leaf water potential at which canopy expansion starts to decrease (Tables 1 and 2). With the HERMES model, at both Jokioinen and Lleida, the genotypic traits of the high-yielding group were characterized by larger thermal time from flowering to maturity and maximum CO_2 assimilation at light saturation (A_{max}), but smaller thermal time from sowing to heading, day-length requirement until heading, and critical threshold value for ratio of actual transpiration and potential transpiration to affect growth during grain filling (Tables 1 and 2). With the MCWLA model, at both Jokioinen and Lleida, the genotypic traits of the high yielding group were characterized by a larger LAI_{max} (opposite to CropSyst), staying green after flowering, maximum transpiration rate, intrinsic quantum efficiency of CO_2 uptake and HI, but a smaller development rate from terminal spikelet initiation to flowering and from flowering to maturity, and lower critical threshold value for ratio of transpiration and potential transpiration to affect growth (Tables 1 and 2). With the MONICA model, at both Jokioinen and Lleida, the genotypic traits of the high-yielding group were characterized by a larger thermal time during grain filling period, LAI and A_{max}, but smaller thermal time before flowering, smaller crop-specific coefficient for evapotranspiration (kc), and smaller critical threshold value for ratio of transpiration and potential transpiration to affect growth (Tables 1 and 2). With the SIMPLACE model, at both Jokioinen and Lleida, the genotypic traits of the high yielding group were characterized by a larger thermal time from sowing to flowering (opposite to CropSyst, HERMES and MONICA) and from flowering to maturity, relative growth rate of LAI during exponential growth, specific leaf area (SLA), light use efficiency (LUE), and longer average time between maturity and harvest (Tables 1 and 2). With the *SiriusQuality* model, at both Jokioinen and Lleida, the genotypic traits of the high yielding group were characterized by a larger thermal time from anthesis to physiological maturity, maximum potential surface area of the penultimate leaf lamina, and LUE, but smaller number of leaves produced after floral initiation. In addition, at Lleida, high yielding group were also characterized by smaller maximum rate of acceleration of leaf senescence in response to soil water deficit, and smaller fraction of transpirable soil water threshold for which the stomatal conductance starts to decrease (Tables 1, 2). With the WOFOST model, at Jokioinen, the genotypic traits of the high yielding group were characterized by a larger thermal time from anthesis to physiological maturity, relative initial leaf growth rate, SLA, maximum leaf assimilation rate, maximum daily increase in rooting depth, maximum rooting depth, and partitioning fraction for storage organs at flowering stage (Table 1). At Lleida, the genotypic traits of the

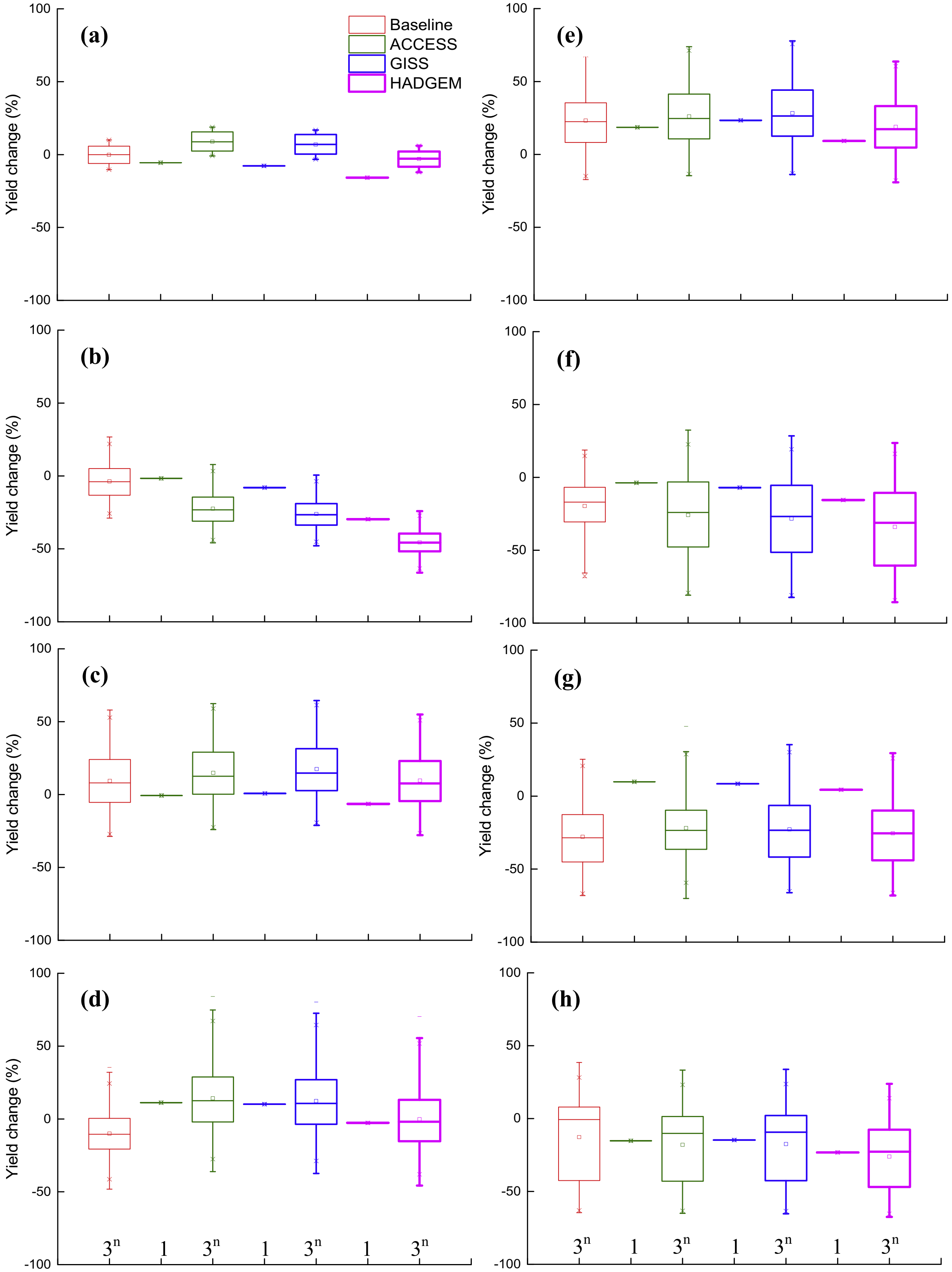

Fig. 3. Box–whisker plots (whisker: minimum and maximum; crosses: 0.01 and 0.99 percentiles; box: 0.25 quartile, median and 0.75 quartile; square: mean) of simulated mean yield changes at Jokioinen, Finland, with 3^n(n is the number of the selected genetic cultivar parameters for a crop model) sets of perturbed genetic cultivar parameters under baseline climate conditions and future climate scenarios, and with one set of calibrated genetic cultivar parameters under future-climate scenarios, relative to the simulations with one set of calibrated genetic cultivar parameters under baseline conditions, using APSIM (a), CropSyst (b), HERMES (c), MCWLA (d), MONICA (e), SIMPLACE (f), *SiriusQuality* (g) and WOFOST (h) crop model.

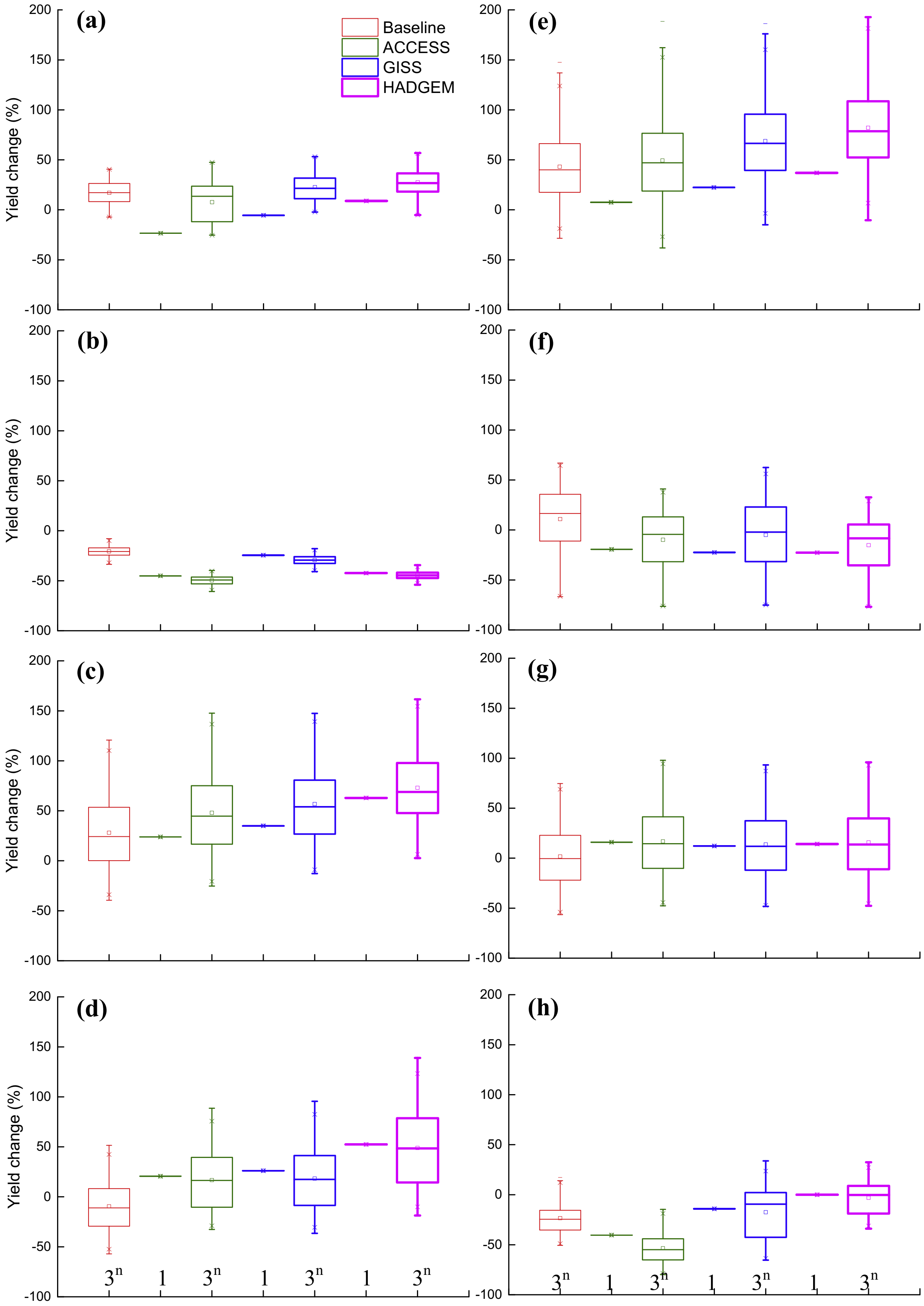

Fig. 4. Same as Fig. 3, except at Lleida, Spain.

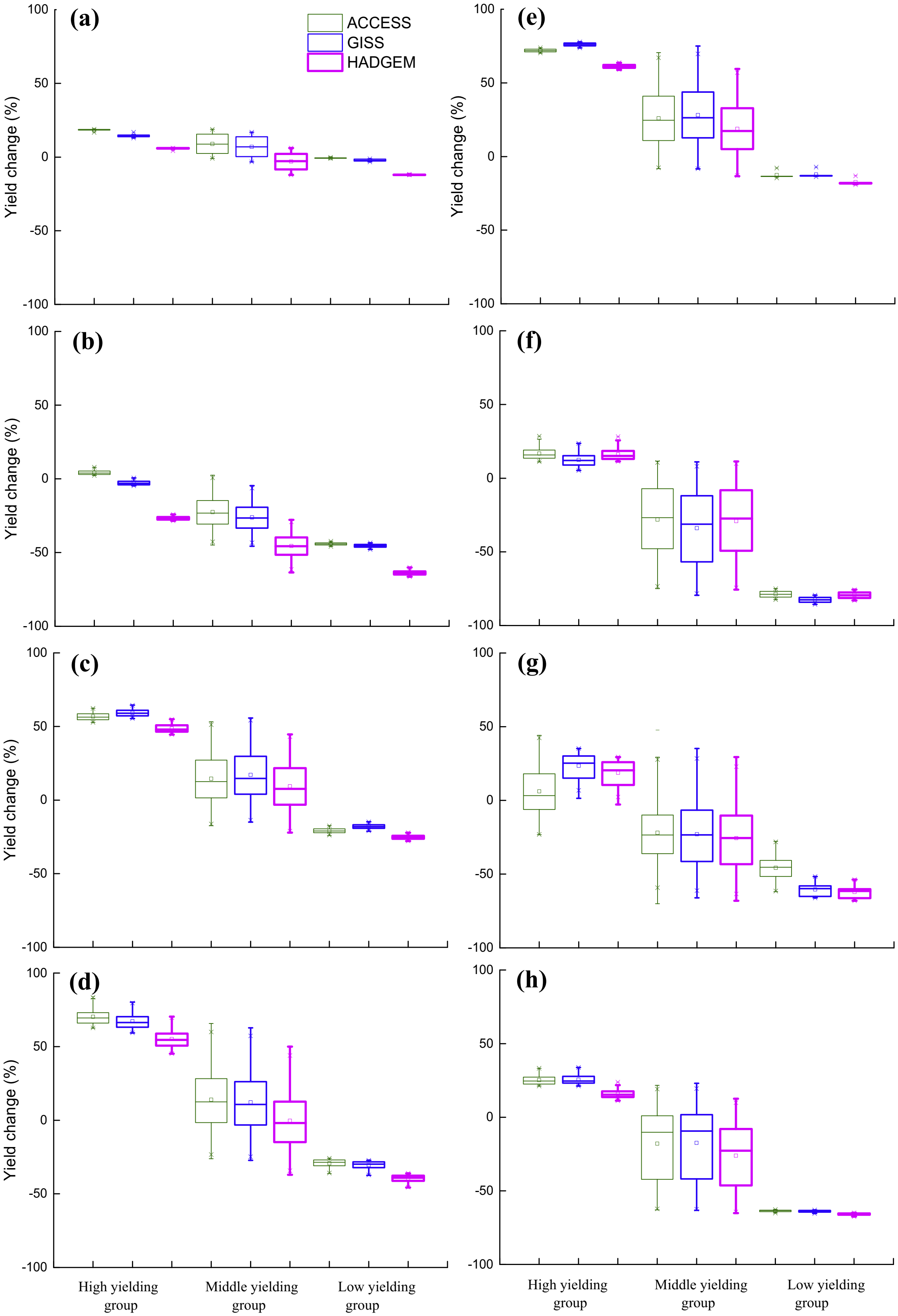

Fig. 5. Box–whisker plots (whisker: minimum and maximum; crosses: 0.01 and 0.99 percentiles; box: 0.25 quartile, median and 0.75 quartile; square: mean) of simulated mean yield changes at Jokioinen, Finland, by the 100 sets of perturbed genetic cultivar parameters that produced the highest mean yield (high yielding group), by the 3^n-100-100 sets (n is the number of the selected genetic cultivar parameters for a crop model) of perturbed genetic cultivar parameters that produced the middle mean yield (middle yielding group), and by the 100 sets of perturbed genetic cultivar parameters that produced the lowest mean yield (low yielding group) under the three future climate scenarios for 2050s, relative to the simulations with one set of calibrated genetic cultivar parameters under baseline conditions, using APSIM (a), CropSyst (b), HERMES (c), MCWLA (d), MONICA (e), SIMPLACE (f), SiriusQuality (g) and WOFOST (h) crop model.

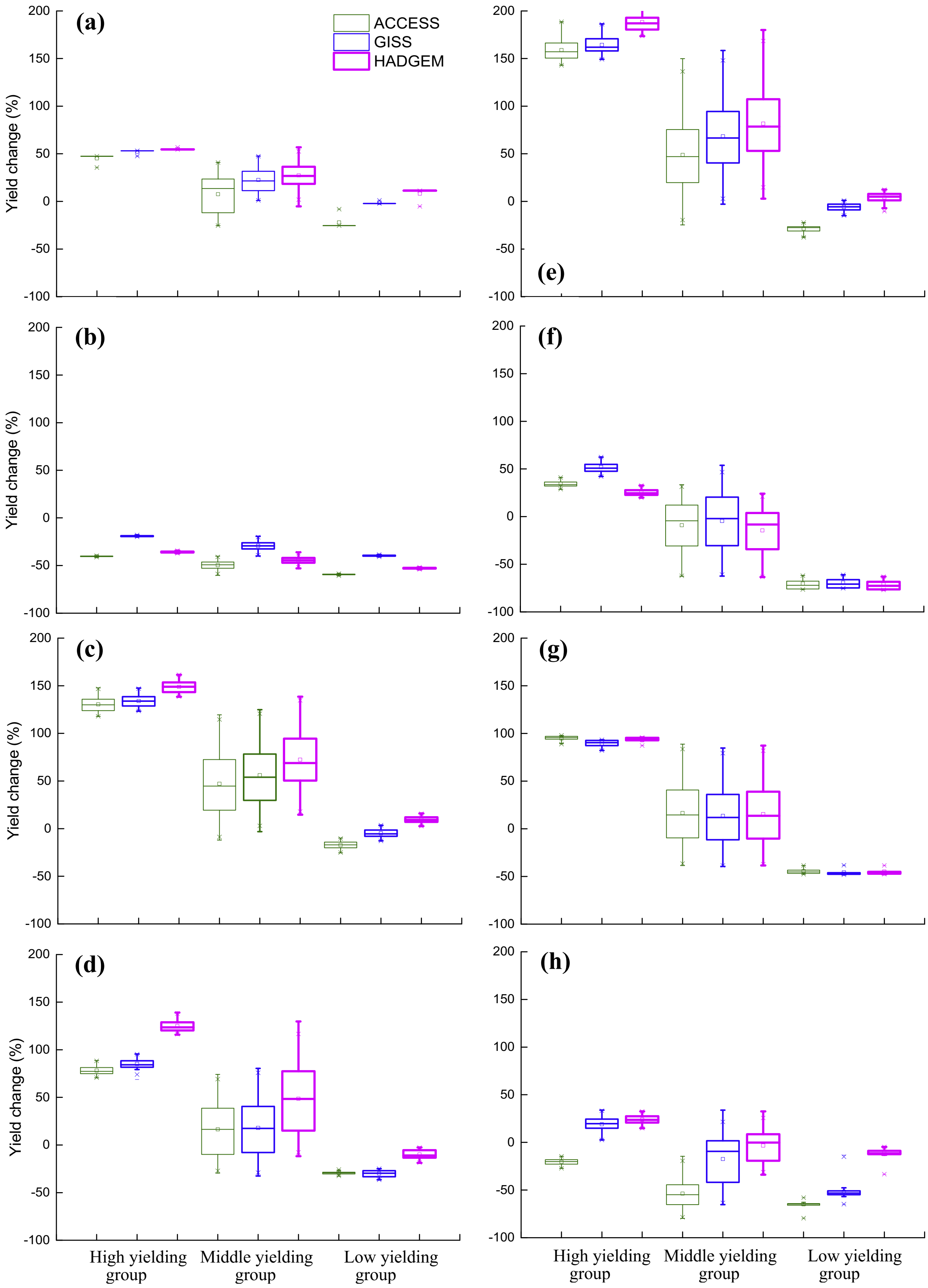

Fig. 6. Same as Fig. 5, except at Lleida, Spain.

Table 1
Mean values and standard deviations (Std) of key cultivar parameters in each crop model for the high-yielding, middle-yielding, and low-yielding groups at Jokioinen, Finland. The calibrated set of cultivar parameters in each crop model is also listed. The value of parameter for high-yielding group is shaded in red (blue) if it is larger (smaller) than those for the middle- and low-yielding groups. (For interpretation of the references to color in this table legend, the reader is referred to the web version of this article.)

		High-yielding group		Middle-yielding group		Low-yielding group		Baseline
	Parameter	Mean	Std	Mean	Std	Mean	Std	Calibrated
APSIM	photop_sens	4.05	0.74	3.48	0.82	3.94	0.62	3.5
	vern_sens	1.29	0.10	1.00	0.27	0.67	0.033	1
	y_node_app_rate (2)	77.75	3.21	74.95	4.08	75.15	4.29	75
	y_rue (3)	1.32	0.00	1.24	0.067	1.16	0.020	1.24
	y_CO$_2$_te_modifier (2)	1.33	0.063	1.37	0.075	1.35	0.068	1.37
	transp_eff_cf (3)	0.006	0.0004	0.006	0.0004	0.006	0.0004	0.006
	max_grain_size	0.10	0.0082	0.10	0.01	0.10	0.0083	0.1
	grains_per_gram_stem	32.48	2.22	32.01	2.17	30.67	1.99	32
CropSyst	GDD_Flw	782.67	16.74	799.75	27.15	833.33	0.00	750
	GDD_Mty	1358.99	27.54	1349.97	27.15	1342.67	27.02	1350
	LAImax	5.99	0.55	6.00	0.54	6.01	0.55	5
	LWP_red	-1281.31	80.15	-1199.85	108.70	-1128.02	87.69	-1200
	RUE	2.82	0.10	2.65	0.19	2.55	0.16	2.8
	C_TB	6.67	0.00	6.20	0.38	5.75	0.08	6.7
	MWU	9.37	0.42	9.00	0.54	8.74	0.49	8.6
	HI	0.57	0.00	0.50	0.054	0.43	0.00	0.53
HERMES	Tsum1	128.40	24.34	135.05	24.41	140.70	25.12	148
	Tsum3	308.33	0.00	425.00	92.86	541.67	0.00	575
	Tsum4	154.67	13.61	155.03	13.62	154.83	13.71	130
	Tsum5	453.33	0.00	360.00	74.28	266.67	0.00	240
	DL	16.96	0.56	18.0	1.08	19.08	0.53	20
	A_{max}	50.72	1.33	50.49	1.36	50.42	1.37	48
	Scr(5)	0.49	0.055	0.50	0.055	0.50	0.054	0.6
MCWLA	R_{maxvg2}	0.029	0.0072	0.038	0.01	0.048	0.0056	0.038
	R_{maxrg}	0.029	0.0013	0.042	0.01	0.055	0.0032	0.042
	L_{AImax}	7.03	0.27	7.00	0.27	6.97	0.27	7
	L_{AIdg}	0.54	0.099	0.50	0.11	0.45	0.10	0.5
	T_{Tmax}	6.75	0.57	5.74	1.08	4.53	0.38	5.74
	α (Intrinsic quantum efficiency of CO$_2$ uptake)	0.085	0.0029	0.08	0.0055	0.076	0.0043	0.08
	S_{cr}	0.49	0.055	0.50	0.054	0.51	0.054	0.47
	HI	0.61	0.0094	0.54	0.054	0.48	0.013	0.54
MONICA	Tsum3	233.33	0.00	300.00	54.01	366.67	0.00	280
	Tsum5	431.00	39.43	349.94	81.36	273.0	48.94	290
	LAI3	0.0025	0.0007	0.0023	0.0007	0.0021	0.0007	0.0019
	A_{max}	46.70	5.33	39.96	8.15	35.80	7.55	30
	kc3	0.68	0.086	0.95	0.24	1.25	0.00	1
	kc5	0.80	0.21	0.95	0.24	1.06	0.22	0.8
	Scr3	0.65	0.19	0.65	0.19	0.66	0.19	0.8
	Scr5	0.48	0.12	0.65	0.19	0.85	0.084	0.6
SIMPLACE	AirTemperatureSumAnthesis	911.68	80.89	855.29	135.84	683.33	0.00	861.5
	AirTemperatureSumMaturity	1509.31	51.47	1394.90	108.14	1392.0	108.54	1440
	RGRL	0.022	0.002	0.02	0.003	0.017	0.00	0.02
	SLA	0.031	0.0026	0.028	0.004	0.024	0.002	0.026
	LUE	3.29	0.079	3.197	0.11	3.17	0.11	3.2
	M2H	0.19	0.074	0.148	0.082	0.15	0.082	0.1
	StartWaterSensitiveDVS	0.84	0.19	0.85	0.19	0.85	0.19	0.85
SiriusQuality	P	132.93	9.58	129.91	10.89	132.53	11.16	135
	Dgf	503.34	26.80	449.81	54.28	408.66	42.14	450
	AreaPL	33.67	5.39	30.02	5.41	24.87	3.89	30
	NLL	4.57	0.39	5.00	0.54	5.50	0.35	5
	LUEDiffuse	4.38	0.00	3.55	0.68	2.72	0.00	4.5
	MaxDSF	3.88	0.67	3.75	0.68	3.71	0.66	4
	UpperFTSWgs	0.50	0.048	0.50	0.055	0.49	0.050	0.5
	BetaRWU	0.074	0.013	0.075	0.014	0.077	0.014	0.07
WOFOST	TSUM1	650.0	25.12	727.49	67.54	641.67	0.00	720
	TSUM2	668.66	21.35	650.06	27.18	627.34	17.65	640
	RGRLAI	0.011	0.0006	0.008	0.0027	0.0047	0.00	0.008
	SLATB	0.0044	0.0007	0.004	0.0009	0.0037	0.0009	0.0035
	A_{max}	35.68	1.54	35.01	1.63	33.84	1.21	35
	RRI	2.90	0.58	2.24	0.95	1.99	0.98	2
	RDMCR	116.67	16.75	99.76	27.27	98.67	27.59	80
	FOTB	0.94	0.031	0.90	0.052	0.84	0.020	0.85

Table 2
Mean values and standard deviations (Std) of key genetic cultivar parameters in each crop model for the high-yielding, middle-yielding, and low-yielding groups at Lleida, Spain. The calibrated set of cultivar parameters in each crop model is also listed. The value of parameter for high yielding group is shaded in red (blue) if it is larger (smaller) than those for the middle- and low-yielding groups. (For interpretation of the references to color in this table legend, the reader is referred to the web version of this article.)

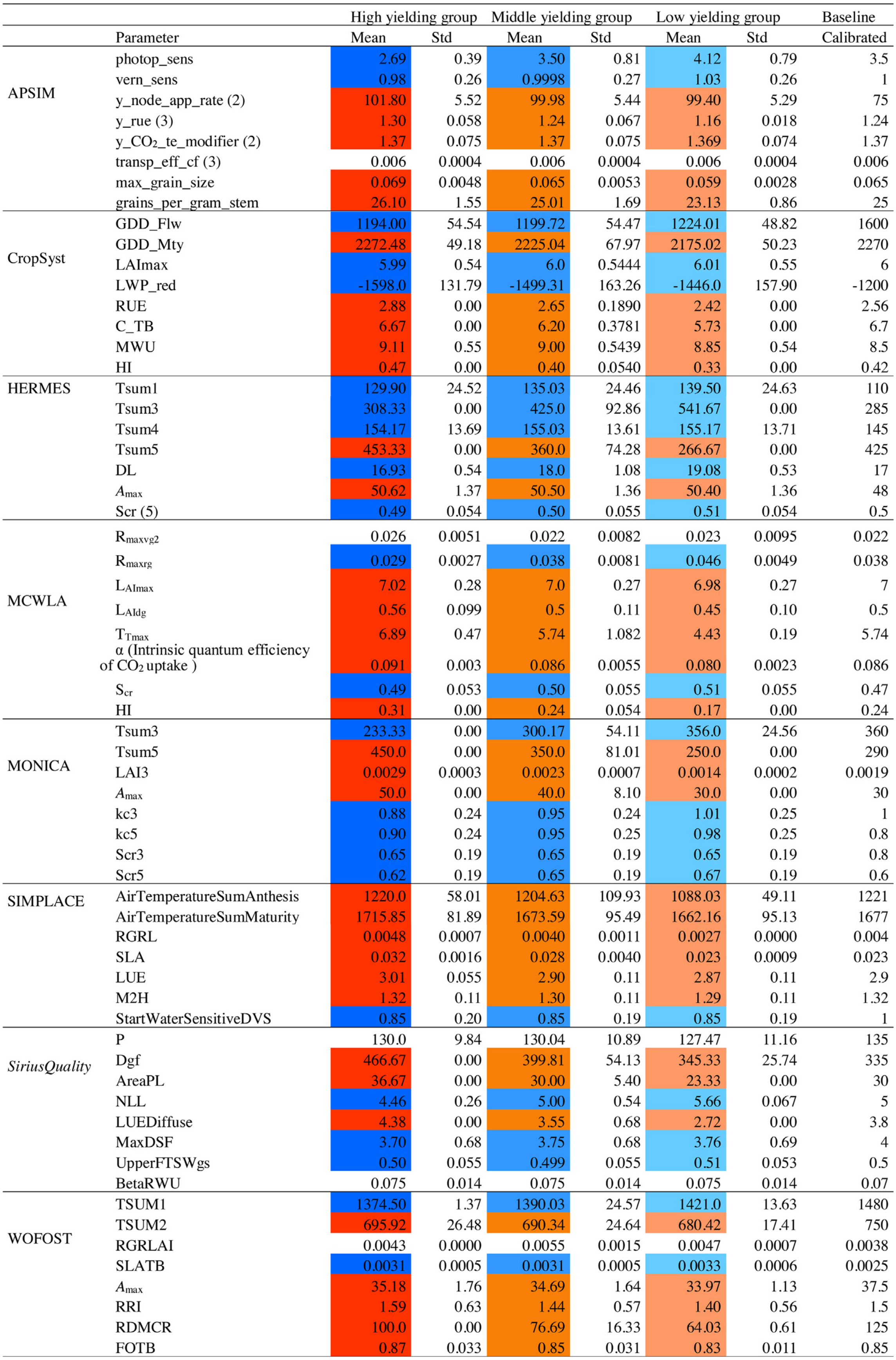

		High yielding group		Middle yielding group		Low yielding group		Baseline
	Parameter	Mean	Std	Mean	Std	Mean	Std	Calibrated
APSIM	photop_sens	2.69	0.39	3.50	0.81	4.12	0.79	3.5
	vern_sens	0.98	0.26	0.9998	0.27	1.03	0.26	1
	y_node_app_rate (2)	101.80	5.52	99.98	5.44	99.40	5.29	75
	y_rue (3)	1.30	0.058	1.24	0.067	1.16	0.018	1.24
	y_CO_2_te_modifier (2)	1.37	0.075	1.37	0.075	1.369	0.074	1.37
	transp_eff_cf (3)	0.006	0.0004	0.006	0.0004	0.006	0.0004	0.006
	max_grain_size	0.069	0.0048	0.065	0.0053	0.059	0.0028	0.065
	grains_per_gram_stem	26.10	1.55	25.01	1.69	23.13	0.86	25
CropSyst	GDD_Flw	1194.00	54.54	1199.72	54.47	1224.01	48.82	1600
	GDD_Mty	2272.48	49.18	2225.04	67.97	2175.02	50.23	2270
	LAImax	5.99	0.54	6.0	0.5444	6.01	0.55	6
	LWP_red	-1598.0	131.79	-1499.31	163.26	-1446.0	157.90	-1200
	RUE	2.88	0.00	2.65	0.1890	2.42	0.00	2.56
	C_TB	6.67	0.00	6.20	0.3781	5.73	0.00	6.7
	MWU	9.11	0.55	9.00	0.5439	8.85	0.54	8.5
	HI	0.47	0.00	0.40	0.0540	0.33	0.00	0.42
HERMES	Tsum1	129.90	24.52	135.03	24.46	139.50	24.63	110
	Tsum3	308.33	0.00	425.0	92.86	541.67	0.00	285
	Tsum4	154.17	13.69	155.03	13.61	155.17	13.71	145
	Tsum5	453.33	0.00	360.0	74.28	266.67	0.00	425
	DL	16.93	0.54	18.0	1.08	19.08	0.53	17
	A_{max}	50.62	1.37	50.50	1.36	50.40	1.36	48
	Scr (5)	0.49	0.054	0.50	0.055	0.51	0.054	0.5
MCWLA	R_{maxvg2}	0.026	0.0051	0.022	0.0082	0.023	0.0095	0.022
	R_{maxrg}	0.029	0.0027	0.038	0.0081	0.046	0.0049	0.038
	L_{AImax}	7.02	0.28	7.0	0.27	6.98	0.27	7
	L_{AIdg}	0.56	0.099	0.5	0.11	0.45	0.10	0.5
	T_{Tmax}	6.89	0.47	5.74	1.082	4.43	0.19	5.74
	α (Intrinsic quantum efficiency of CO_2 uptake)	0.091	0.003	0.086	0.0055	0.080	0.0023	0.086
	S_{cr}	0.49	0.053	0.50	0.055	0.51	0.055	0.47
	HI	0.31	0.00	0.24	0.054	0.17	0.00	0.24
MONICA	Tsum3	233.33	0.00	300.17	54.11	356.0	24.56	360
	Tsum5	450.0	0.00	350.0	81.01	250.0	0.00	290
	LAI3	0.0029	0.0003	0.0023	0.0007	0.0014	0.0002	0.0019
	A_{max}	50.0	0.00	40.0	8.10	30.0	0.00	30
	kc3	0.88	0.24	0.95	0.24	1.01	0.25	1
	kc5	0.90	0.24	0.95	0.25	0.98	0.25	0.8
	Scr3	0.65	0.19	0.65	0.19	0.65	0.19	0.8
	Scr5	0.62	0.19	0.65	0.19	0.67	0.19	0.6
SIMPLACE	AirTemperatureSumAnthesis	1220.0	58.01	1204.63	109.93	1088.03	49.11	1221
	AirTemperatureSumMaturity	1715.85	81.89	1673.59	95.49	1662.16	95.13	1677
	RGRL	0.0048	0.0007	0.0040	0.0011	0.0027	0.0000	0.004
	SLA	0.032	0.0016	0.028	0.0040	0.023	0.0009	0.023
	LUE	3.01	0.055	2.90	0.11	2.87	0.11	2.9
	M2H	1.32	0.11	1.30	0.11	1.29	0.11	1.32
	StartWaterSensitiveDVS	0.85	0.20	0.85	0.19	0.85	0.19	1
SiriusQuality	P	130.0	9.84	130.04	10.89	127.47	11.16	135
	Dgf	466.67	0.00	399.81	54.13	345.33	25.74	335
	AreaPL	36.67	0.00	30.00	5.40	23.33	0.00	30
	NLL	4.46	0.26	5.00	0.54	5.66	0.067	5
	LUEDiffuse	4.38	0.00	3.55	0.68	2.72	0.00	3.8
	MaxDSF	3.70	0.68	3.75	0.68	3.76	0.69	4
	UpperFTSWgs	0.50	0.055	0.499	0.055	0.51	0.053	0.5
	BetaRWU	0.075	0.014	0.075	0.014	0.075	0.014	0.07
WOFOST	TSUM1	1374.50	1.37	1390.03	24.57	1421.0	13.63	1480
	TSUM2	695.92	26.48	690.34	24.64	680.42	17.41	750
	RGRLAI	0.0043	0.0000	0.0055	0.0015	0.0047	0.0007	0.0038
	SLATB	0.0031	0.0005	0.0031	0.0005	0.0033	0.0006	0.0025
	A_{max}	35.18	1.76	34.69	1.64	33.97	1.13	37.5
	RRI	1.59	0.63	1.44	0.57	1.40	0.56	1.5
	RDMCR	100.0	0.00	76.69	16.33	64.03	0.61	125
	FOTB	0.87	0.033	0.85	0.031	0.83	0.011	0.85

high yielding group were characterized by larger thermal time from anthesis to physiological maturity, maximum leaf assimilation rate, maximum daily increase in rooting depth, maximum rooting depth, and partitioning fraction for storage organs at DVS 1.01, but smaller thermal time before anthesis, and smaller SLA (Table 2). The ideotypic traits identified by most of the crop models were consistent for Jokioinen (Table 1) and Lleida (Table 2). Only APSIM and WOFOST showed differences in favorable traits at these two sites.

3.6. Proposed barley ideotypes for future climate based on crop model ensemble

Climate-resilient and high-yielding barley ideotypes under future climate scenarios are proposed separately for Boreal (Table 3) and Mediterranean climate (Table 4), by combining the ideotypic traits identified by the crop model ensemble. In terms of phenology, seven models, CropSyst, HERMES, MCWLA, MONICA, SIMPLACE, *SiriusQuality*, and WOFOST, suggest that successful barley ideotypes should have a larger thermal time from anthesis to physiological maturity. Three models, CropSyst, HERMES, and MONICA, suggest that barley ideotypes should have a smaller thermal time before anthesis (Tables 3 and 4). Furthermore, optimal barley ideotypes should have a smaller photoperiod (according to HERMES) and higher vernalization sensitivity (according to APSIM) at Jokioinen (Table 3), but a smaller photoperiod (according to APSIM and HERMES) and vernalization sensitivity (according to APSIM) at Lleida (Table 4). Regarding leaf area, four models, MCWLA, MONICA, SIMPLACE, and *SiriusQuality*, suggest that barley ideotypes should have a larger SLA and $\mathrm{LAI}_{\max}$ with a lower senescence rate at both Jokioinen and Lleida (Tables 3 and 4). However, there was not full agreement among the crop models. For example, CropSyst suggests a smaller maximum LAI at both Jokioinen and Lleida (Tables 3 and 4); WOFOST suggests a larger leaf growth rate and SLA at Jokioinen, but a smaller SLA at Lleida (Table 4). For photosynthesis, all eight models suggest that climate-resilient barley ideotypes should have a larger $A_{\max}$ or RUE at both Jokioinen and Lleida (Tables 3 and 4). In terms of drought tolerance, five models, CropSyst, HERMES, MCWLA, MONICA, and WOFOST, suggest that climate-resilient barley ideotypes should have a higher water use efficiency, drought tolerance, and maximum rooting depth (Tables 3 and 4). In comparison with Jokioinen, drought-resistant traits are even more beneficial at Lleida. Regarding grain formation, four models, APSIM, CropSyst, MCWLA, and WOFOST, suggest that barley ideotypes should have a larger grain number, grain size, and HI at both Jokioinen and Lleida (Tables 3 and 4).

4. Discussion

4.1. Use of an ensemble of crop models in ideotypes design

Plant breeding focuses on developing superior genotypes with available genetic and non-genetic resources and improved plant-breeding methods to maximize genetic gain and cost-effectiveness. Computer simulation of crop growth can lay out the breeding process in silico and identify optimal candidate genotypes for various future scenarios; empirical validation can then follow and be refined after various iterations (Li et al., 2012; Rötter et al., 2015). The current study demonstrates a key component of a sound collaborative approach (Rötter et al., 2015) to design future climate-resilient barley ideotypes aided by crop growth simulation and, for the first time, an ensemble modelling approach. The strengths of the latter for crop modelling have recently been discussed by Wallach et al. (2016) and include, among others, better predictive skills of the ensemble median or mean as compared to single models and the possibility to provide measures of confidence regarding model results.

Our approach has clear advantages over previous studies using one single crop model and/or focusing on one single cultivar trait. The crop models applied in this study are all well tested for Europe but quite different in terms of the number of processes included and their descriptions, complexity, and cultivar parameters (Asseng et al., 2013). Nevertheless, the cultivar parameters in each crop model are closely related to the processes that are common to all models such as crop growth, root and leaf development, photosynthesis, evapotranspiration, abiotic stress, and grain formation. Results from such an ensemble are more reliable than the results from a single model, because possible artefacts due to the poor structure of a single model are levelled or minimized by using ensembles, which are generally based and validated on a larger pool of data (Martre et al., 2015b; Wallach et al., 2016).

The crop models included in our ensemble consistently showed that some traits would be promising under future climate change scenarios, which led to more robust identification of crop ideotypes. Furthermore, the different modelling approaches, complexity, and cultivar parameters among the models have complementary roles in identification of crop ideotypes, which increases the robustness of the results. For example, CropSyst and MCWLA identify a larger HI, WOFOST identifies a larger partitioning fraction for storage organs, and APSIM identifies a larger grain number and grain weight as the desirable ideotypic traits. There are obvious shortcomings from relying on any single model compared to the ensemble. For instance, CropSyst suggests a smaller $\mathrm{LAI}_{\max}$ at Jokioinen, which is contrary to the other five models (MCWLA, MONICA, SIMPLACE, *SiriusQuality* and WOFOST). In such cases, the results shared by multiple models were adopted in this study unless there was a known problem (e.g., systematic bias regarding a certain process) that made an ensemble of models inferior to a single (best) model (Tebaldi and Knutti, 2007).

For crop model parameters, their value ranges and how they were sampled for the perturbation runs could affect the magnitude of the simulated yield change, but the general conclusions on ideotypes design would not be affected and remain sound. However, the approach also has some limitations due to particular uncertainties. For example, the representation of the complex interactions between traits and between processes is not yet fully understood and therefore not completely represented in current crop models (Boote et al., 2001). Moreover, the trade-offs and associations between genotypic traits are insufficiently known (Martre et al., 2007) and have not been fully taken into account in this study. This implies that all the ideotypic traits we identified might not be simultaneously and perfectly realized by breeders without compromise. Nevertheless, the proposed ideotypes based on results from an ensemble of models serves as the first step towards figuring out crop ideotypic traits for breeders to develop future climate resilient crop cultivars. With the proposed ideotypic traits as breeding target, the insights from the study are potentially meaningful for genotype development programs. For instance, in order to realize the ideotypic trait of drought tolerance, breeders may focus on the model-identified plant traits such as maximum daily increase in rooting depth, maximum rooting depth, critical threshold value for ratio of actual transpiration and potential transpiration, crop evapotranspiration coefficient, and transpiration efficiency.

4.2. Ecophysiological basis of the ideotypic traits

The ideotypic traits identified in this study have a sound ecophysiological basis and an excellent track record in promoting crop productivity in the past few decades. Barley ideotypes should have a lower photoperiod sensitivity and larger vernalization sensitivity at Jokioinen, and lower photoperiod sensitivity and smaller

Table 3
Identify barley ideotypes for Jokioinen under future climate conditions based on the crop model ensemble.

	Ideotypic traits	APSIM	CropSyst	HERMES	MCWLA	MONICA	SIMPLACE	*SiriusQuality*	WOFOST
Phenology	① Larger thermal time from anthesis to physiological maturity		Larger GDD_Mty	Larger Tsum5	Smaller R_{maxrg}	Larger Tsum5	Larger AirTemperatureSumMaturity	Larger Dgf	Larger TSUM2
	② Smaller thermal time before anthesis		Smaller GDD_Flw	Smaller Tsum1 and Tsum3		Smaller Tsum3			
	③ Smaller photoperiod and larger vernalization sensitivity	Larger vern_sens		Smaller DL					
Leaf area	① Larger SLA and maximum LAI				Larger L_{AImax}	Larger LAI3	Larger RGRL and SLA	Larger AreaPL	Larger RGRLAI and SLATB
	② Lower senescence rate				Larger L_{AIdg}				
Photosynthesis	① Larger A_{max} or RUE	Larger y_rue	Larger RUE	Larger A_{max}	Larger α	Larger A_{max}	Larger RUE	Larger LUEDiffuse	Larger A_{max}
Drought tolerance	① Higher water use efficiency		Larger C_TB			Smaller kc			
	② Higher drought tolerance			Smaller Scr	Smaller Scr	Smaller Scr			
	③ Larger maximum rooting depth		Larger MWU						Larger RRI and RDMCR
Grain formation	① Larger grain number	Larger grains_per_gram_stem							
	② Larger HI		Larger HI		Larger HI				Larger FOTB

Table 4
Identify barley ideotypes for Lleida under future climate conditions based on the crop model ensemble.

	Ideotypic traits	APSIM	CropSyst	HERMES	MCWLA	MONICA	SIMPLACE	*SiriusQuality*	WOFOST
Phenology	① Larger thermal time from anthesis to physiological maturity		Larger GDD_Mty	Larger Tsum5	Smaller R_{maxrg}	Larger Tsum5	Larger AirTemperatureSumMaturity	Larger Dgf	Larger TSUM2
	② Smaller thermal time before anthesis		Smaller GDD_Flw	Smaller Tsum1, Tsum2 and Tsum3		Smaller Tsum3			Smaller TSUM1
	③ Smaller photoperiod and vernalization sensitivity	Smaller photop_sens and vern_sens		Smaller DL					
Leaf area	① Larger SLA and maximum LAI				Larger L_{AImax}	Larger LAI3	Larger RGRL and SLA	Larger AreaPL	
	② Lower senescence rate				Larger L_{AIdg}				
Photosynthesis	① Larger A_{max} or RUE	Larger y_rue	Larger RUE	Larger A_{max}	Larger α	Larger A_{max}	Larger RUE	Larger LUEDiffuse	Larger A_{max}
Drought tolerance	① Higher water use efficiency		Larger C_TB			Smaller kc			
	② Higher drought tolerance			Smaller Scr	Smaller Scr	Smaller Scr			
	③ Larger maximum rooting depth								Larger RRI and RDMCR
Grain formation	① Larger grain number	Larger grains_per_gram_stem							
	② Larger grain size	Larger max_grain_size							
	③ Larger HI		Larger HI		Larger HI				Larger FOTB

vernalization sensitivity at Lleida. At Jokioinen, lower photoperiod sensitivity increases the duration of stem elongation phase, larger vernalization sensitivity increases the duration from emergence to terminal spikelet initiation, which stimulates flowering, enhances seed production and reduces climate risk (Dennis and Peacock, 2009). At Lleida, lower photoperiod sensitivity and smaller vernalization sensitivity increases the duration of stem elongation phase, which leads to a higher number of fertile florets at anthesis, an increased grain number and thereby a higher yield (González et al., 2003; Miralles and Richards, 2000). Extending the phase of stem elongation has been proposed as a tool to further improve yield potential in small-grain cereals (Borràs-Gelonch et al., 2010; Miralles and Richards, 2000). Vernalization response is different at each location because Jokioinen benefits from a large vegetative/reproductive ratio that assures flowering occurs only once mild season has begun; at Lleida, where such a risk is much lower, a smaller ratio implies a longer grain filling and therefore higher yield.

Barley ideotypes should have a larger reproductive growth duration and shorter pre-anthesis duration. The duration of the grain filling period is positively correlated with grain weight (Fernández et al., 1998) and has common genetic determinants in wheat (Charmet et al., 2005). Cultivars with longer reproductive growth duration have been increasingly adopted to take advantage of increased temperatures in autumn due to climate change at high latitudes. At lower latitudes, increases in the grain filling period (actually the increase in the thermal requirement) allow the crop to maintain (even in a warmer environment) the duration of grain filling. Also, selection of early-heading crop genotypes secures higher yields because cultivars with earlier heading dates usually have longer grain filling period and also escape more severe terminal water stress, for example, in Southwest Texas (Fernández et al., 1998) and China (Tao et al., 2012). However, care should be taken that shortening of the pre-anthesis period does not lead to reduction in the duration of ear formation, which may be challenging but nevertheless possible (Foulkes et al., 2011).

Barley ideotypes should have a larger leaf area but a smaller leaf senescence rate in response to heat and water stress. An increase in leaf area increases light interception and the source strength for heat, water and CO_2 exchange, and consequently increases photosynthesis rate and biomass accumulation. However, in dry environments with terminal drought, it could also have negative effects on yield if water is depleted too early in the season: for this reason models CropSyst and WOFOST suggested a smaller leaf area at Lleida. Barley productivity can be limited by both water and heat stress, which hasten premature senescence and consequently lower yield. Lower leaf senescence rate or 'staying green' is a vital characteristic associated with the capacity of the plant to maintain CO_2 assimilation and photosynthesis, which mostly results from other traits such as a higher proportion of roots in deep soil (Borrell et al., 2001).

Barley ideotypes should have a larger A_{max} and RUE. The amount of radiation captured will determine the rate of photosynthesis possible and the rate of growth (the rate of the accumulation of dry matter). Past increases in yield potential of wheat have largely resulted from improvements in HI rather than increased biomass. Further increases in HI are relatively difficult than before, but an opportunity exists for increasing productive biomass and harvestable grain. Photosynthetic capacity and efficiency are bottlenecks to raising productivity and there is strong evidence that increasing photosynthesis will increase crop yields provided that other constraints do not become limiting (Parry et al., 2010). Moreover, barley ideotypes should have a higher water use efficiency, drought tolerance, and maximum rooting depth, which are essential to meet the challenge of maintaining yields while facing increasing drought risk due to climate change. Improved water use efficiency for grain in modern cultivars was associated with faster development, earlier flowering, improved canopy structure, and higher HI (Siddique et al., 1990). Finally, barley ideotypes should have a larger grain number, grain size, and HI. It is therefore crucial to optimize partitioning of extra assimilates to grain to maximize grain number and HI, and to improve potential grain size and grain filling while maintaining lodging resistance (Foulkes et al., 2011).

In the past several decades in Finland, drought, excess of water from rain and snow-melt, as well as high temperature sum accumulation rate before heading, severely reduced barley yields, while high temperature sum accumulation rate from heading to yellow ripeness increased the yields significantly (Hakala et al., 2012). In addition, increased grain number, grain size, and consequently HI have contributed to genetic yield improvements in spring barley (*Hordeum vulgare* L.), oat (*Avena sativa* L.), and wheat (*Triticum aestivum* L.) cultivars (Peltonen-Sainio et al., 2007). In the Mediterranean basin, modern cultivars used slightly less water than old cultivars. Water use efficiency for grain has increased substantially from old to modern cultivars for wheat and barley (Siddique et al., 1990; Shearman et al., 2005; Acreche and Slafer, 2009; Bustos et al., 2013). The proposed barley ideotypes with high water use efficiency (larger C_TB and smaller kc), high drought tolerance (smaller Scr) and large maximum rooting depth (larger RRI and RDMCR) would help to combat the abiotic stress and increase genetic gains under future climate conditions.

4.3. Implications of this study to climate impact and adaptation studies, as well as to agronomists and breeders

This study showed that barley yield could increase substantially under future climate scenarios if new ideotypes are developed and implemented, which is in contrast with many previous climate change impact studies that did not consider genotypic adaptations (see, e.g., Challinor et al., 2014 for an overview). The potential effect of unleashing crop breeding and biotechnology to combat climate change impacts such as food supply reductions is overlooked in many climate impacts studies, including IPCC AR5 (Zilberman, 2015). Rötter et al. (2011a) concluded that positive effects of climate warming and elevated CO_2 concentrations on cereal production at high latitudes are likely to be reversed for temperature increases exceeding 4 °C, with a high risk of marked yield loss. The same authors also suggested that only plant breeding efforts aimed at increasing both yield potential and drought tolerance, combined with adjusted agronomic practices, such as changed sowing time, adequate nitrogen fertilizer management and plant protection, hold a prospect of maintaining yield levels and reducing the risks of yield shortfall. Responding to climate change will therefore require the use of new breeding methods to create suitable genotypes (Dawson et al., 2015). In Spain, a shift in adapted cereal-based crop rotations is expected where a summer crop becomes a winter-sown crop (Garrido et al., 2011). In order to better predict future climate impacts on food production and food security, the development of agronomic management and new genotypes should be elaborated and incorporated into future climate change impact and adaptation studies.

Furthermore, our study demonstrates a sound approach to accelerate collaboration among crop modellers, agronomists, physiologists, geneticists, and breeders, which is extremely important but surprisingly rare so far (Rötter et al., 2015). The traits identified in our study have important implications for these experts' efforts to develop climate-resilient crop cultivars. In more comprehensive studies and programmes aimed at accelerating plant breeding for future conditions through collaborative modelling and experiments and by using high-throughput phenotyping technology, the identified value ranges for various crop model parameters can be further refined. The genetic basis of the ideotypic traits requires further investigation to accelerate climate-resilient barley cultivars breeding. Moreover, combining conventional crop simulation with genetic modelling, such as based on quantitative trait loci (QTLs) (Yin et al., 2005; Li et al., 2012), promises to accelerate delivery of future cereal cultivars for different environments. The robustness of model-aided ideotypes design can be enhanced further by continuously improving crop models to better account for key physiological processes, cultivar traits, and their interactions, such as three-dimensional canopy structure, heat, frost, and waterlogging resistance, as well as for the interactions between genotype (G), management (M) and environment (E).

5. Conclusions

We developed a new approach to design future crop ideotypes using crop model ensembles and applied it to design climate-resilient barley ideotypes for Boreal and Mediterranean climatic zones in Europe. The study demonstrates a key component of a sound collaborative approach to design future climate-resilient barley ideotypes aided by crop simulation and, for the first time, based on a crop model ensemble. The approach has advantages over previous studies using one single crop model and/or focusing on one single cultivar trait. The results show that barley ideotypes under future climate conditions should have a longer reproductive growing period, lower leaf senescence rate, larger radiation use efficiency or maximum assimilation rate, and higher drought-tolerance for both Boreal and Mediterranean climatic zones. Moreover, barley ideotypes should have a high photoperiod and vernalization sensitivity for the Boreal climatic zone; in contrast they should have a low photoperiod and low vernalization sensitivity for Mediterranean climatic zone. The drought tolerance trait is more beneficial for the Mediterranean climatic zone than for the Boreal climatic zone. The proposed ideotypes for the Boreal and Mediterranean climatic zones have solid ecophysiological bases and an excellent prognosis in promoting crop productivity under ongoing climate change. The insights from the study are potentially meaningful for genotype development programs, which can serve as the first step towards identifying crop ideotypic traits for breeders developing crop cultivars having resilience to projected future climates. The robustness of model-aided ideotype design can be further enhanced through continuously improving crop models and enhancing information exchange between modellers, agrometeorologists, geneticists, physiologists, and plant breeders.

Acknowledgements

The present study was carried out in the context of CropM within the FACCE-MACSUR knowledge hub (031A103B). FT, TP and RPR were supported by the Ministry of Agriculture and Forestry (FACCE-MACSUR) and by the Academy of Finland, the NORFASYS project (decision nos. 268277 and 292944) and PLUMES project (decision nos. 277403 and 292836). MIM, LR and MRR (CEIGRAM-UPM) were supported by MULCLIVAR CGL2012-38923-C02-02 from MINECO. HH, TG and FE were financially supported by the German Federal Ministry of Food and Agriculture (BMEL) through the Federal Office for Agriculture and Food (BLE), (2851ERA01J) and thank Andreas Enders and Gunther Krauss (INRES, University of Bonn) for support. KCK and CN were supported by German Ministry of Education and Research (BMBF), 031B0039C. AD and PM were supported by the European Union's Seventh Framework Programme (FP7/2007–2013; grant no. FP7-613556) and the FACCE-MACSUR project (031A103B) through the metaprogram on Adaptation of Agriculture and Forests to Climate Change (AAFCC) of the French National Institute for Agricultural Research (INRA). The work of AHS was carried out under the FACCEJPI project ClimBar (Academy of Finland project) (284987). Financial support from these projects is gratefully acknowledged.

Appendix A. Supplementary data

Supplementary data associated with this article can be found, in the online version, at http://dx.doi.org/10.1016/j.eja.2016.10.012.

References

Acreche, M.M., Slafer, G.A., 2009. Grain weight: radiation interception and use efficiency as affected by sink-strength in Mediterranean wheats released from 1940 to 2005. Field Crops Res. 110, 98–105.

Addiscott, T.M., Whitmore, A.P., 1991. Simulation of solute leaching in soils with different permeabilities. Soil Use Manage. 7, 94–102.

Asseng, S., Ewert, F., Rosenzweig, C., Jones, J.W., et al., 2013. Uncertainty in simulating wheat yields under climate change. Nat. Clim. Change 3, 827–832.

Asseng, S., Ewert, F., Martre, P., Rötter, R.P., et al., 2015. Rising temperatures reduce global wheat production. Nat. Clim. Change 5, 143–147.

Bassu, S., Brisson, N., Durand, J.L., Boote, K., et al., 2014. How do various maize crop models vary in their responses to climate change factors? Global Change Biol. 20, 2301–2320.

Bergez, E., Colbach, N., Crespo, O., Garcia, F., Jeuffroy, M.H., Justes, E., Loyce, C., Munier-Jolain, N., Sadok, W., 2010. Designing crop management systems by simulation. Eur. J. Agron. 32, 3–9.

Boogaard, H.L., Van Diepen, C.A., Rötter, R.P., Cabrera, J.C.M.A., Van Laar, H.H., 1998. User's guide for the WOFOST 7.1 crop growth simulation model and WOFOST control center 1.5. In: Technical Document 52. Winand Staring Centre, Wageningen, The Netherlands, 144pp.

Boote, K.J., Kropff, M.J., Bindraban, P.S., 2001. Physiology and modelling of traits in crop plants: implications for genetic improvement. Agric. Syst. 70, 395–420.

Borràs-Gelonch, G., Slafer, G.A., Casas, A.M., van Eeuwijk, F., Romagosa, I., 2010. Genetic control of pre-heading phases and other traits related to development in a double-haploid barley (Hordeum vulgare L.) population. Field Crops Res. 119, 36–47.

Borrell, A., Hammer, G., van Oosterom, E., 2001. Stay-green: a consequence of the balance between supply and demand for nitrogen during grain filling? Ann. Appl. Biol. 138, 91–95.

Brisson, N., Gate, P., Gouache, D., Charmet, G., Oury, F.X., Huard, F., 2010. Why are wheat yields stagnating in Europe? A comprehensive data analysis for France. Field Crops Res. 119, 201–212.

Bustos, D.V., Hasan, A.K., Reynolds, M.P., Calderini, D.F., 2013. Combining high grain number and weight through a DH-population to improve grain yield potential of wheat in high-yielding environments. Field Crops Res. 145, 106–115.

Cantero-Martinez, C., Angas, P., Lampurlanes, J., 2003. Growth, yield and water productivity of barley (Hordeum vulgare L.) affected by tillage and N fertilization in Mediterranean semiarid, rainfed conditions of Spain. Field Crops Res. 84, 341–357.

Challinor, A.J., Watson, J., Lobell, D.B., Howden, S.M., Smith, D.R., Chhetri, N., 2014. A meta-analysis of crop yield under climate change and adaptation. Nat. Clim. Change 4, 287–291.

Charmet, G., Robert, N., Branlard, G., Linossier, L., Martre, P., Triboi, E., 2005. Genetic analysis of dry matter and nitrogen accumulation and protein composition in wheat kernels. Theor. Appl. Genet. 111, 540–550.

Dawson, I.K., Russell, J., Powell, W., Steffenson, B., Thomas, B., Waugh, R., 2015. Barley: a translational model for adaptation to climate change. New Phytol. 206, 913–931.

Dennis, E.S., Peacock, W.J., 2009. Vernalization in cereals. J. Biol. 8, 57.

Dingkuhn, M., Penning de Vries, F.W.T., De Datta, S.K., van Laar, H.H., 1991. Concepts for a new plant type for direct seeded flooded tropical rice. In: Direct Seeded Flooded Rice in the Tropics. International Rice Research Institute, P.O. Box 933, M Philippines, pp. 17–38.

Dingkuhn, M., Laza, M.R.C., Kumar, U., Mendez, K.S., Collard, B., Jagadish, K., Singh, R.K., Padolina, T., Malabayabas, M., Torres, E., Rebolledo, M.C., Manneh, B., Sow, A., 2015. Improving yield potential of tropical rice: achieved levels and perspectives through improved ideotypes. Field Crops Res. 182, 43–59.

Dumont, B., Basso, B., Bodson, B., Destain, J.P., Destain, M.F., 2015. Climatic risk assessment to improve nitrogen fertilisation recommendations: a strategic crop model-based approach. Eur. J. Agron. 65, 10–17.

Ewert, F., Rötter, R.P., Bindi, M., Webber, H., et al., 2015. Crop modelling for integrated assessment of risk to food production from climate change. Environ. Modell. Sofw. 72, 287–303.

FAO, 2010. Climate-Smart Agriculture—Policies, Practices and Financing for Food Security, Adaptation and Mitigation.

Fernández, C.J., Tewolde, H., Elledge, R., Foutz, T., 1998. Early-heading winter wheat varieties secure higher yields in southwest texas. BL-RC18. In: Bottom Lines: An Overview of Research and Extension Projects. Texas A&M University Agricultural Research and Extension Center. The Texas Agricultural Experiment Station. The Texas A&M University System, Uvalde, TX.

Foulkes, J., Slafer, G.A., Davies, W.J., Berry, P., Sylvester-Bradley, R., Martre, P., Calderini, D.F., Griffiths, S., Reynolds, M., 2011. Raising yield potential of wheat. III. Optimizing partitioning to grain while maintaining lodging resistance. J. Exp. Bot. 62, 469–486.

Garrido, A., Rey, D., Ruiz-Ramos, M., Mínguez, M.I., 2011. Climate change and crop adaptation in Spain: consistency of regional climate models. Clim. Res. 49, 211–227.

Gerland, P., Raftery, A.E., Ševčíková, H., Li, N., Gu, D., Spoorenberg, T., Alkema, L., Fosdick, B.K., Chunn, J., Lalic, N., Bay, G., Buettner, T., Heilig, G.K., Wilmoth, J., 2014. World population stabilization unlikely this century. Science 346, 234–237.

Godfray, H.C.J., Beddington, J.R., Crute, I.R., Haddad, L., Lawrence, D., et al., 2010. Food security: the challenge of feeding 9 billion people. Science 327, 812–818.

González, F.G., Slafer, G.A., Miralles, D.J., 2003. Grain and floret number in responseto photoperiod during stem elongation in fully and slightly vernalized wheats. Field Crops Res. 81, 17–27.

Gouache, D., Bogard, M., Pegard, M., Thepot, S., Garcia, C., Hourcade, D., Paux, E., Oury, F., Rousset, M., Deswarte, J., Bris, X., 2016. Bridging the gap between ideotype and genotype: challenges and prospects for modelling as exemplified by the case of adapting wheat (Triticum aestivum L.) phenology to climate change in France. Field Crops Res., http://dx.doi.org/10.1016/j.fcr.2015.12.012.

Grassini, P., Eskridge, K.M., Cassman, K.G., 2013. Distinguishing between yield advances and yield plateaus in historical crop production trends. Nat. Commun. 4, 2918, http://dx.doi.org/10.1038/ncomms3918.

Hakala, K., Jauhiainen, L., Himanen, S.J., Rötter, R.P., Salo, T., Kahiluoto, H., 2012. Sensitivity of barley varieties to weather in Finland. J. Agric. Sci. 150, 145–160.

Hatfield, J.L., Boote, K.J., Kimball, B.A., Izaurralde, R.C., Ort, D., Thomson, A., Wolfe, D.W., 2011. Climate impacts on agriculture: implications for crop production. Agron. J. 103, 351–370.

IUSS, 2006. World reference base for soil resources 2006. In: World Soil Resources Reports No. 103. FAO, Rome, Italy.

Iman, R.L., Helton, J.C., Campbell, J.E., 1981. An approach to sensitivity analysis of computer models, part 1. Introduction, input variable selection and preliminary variable assessment. J. Qual. Technol. 13, 174–183.

Jones, C.D., Hughes, J.K., Bellouin, N., Hardiman, S.C., et al., 2011. The HadGEM2-ES implementation of CMIP5 centennial simulations. Geosci. Model Dev. 4, 543–570.

Keating, B.A., Carberry, P.S., Hammer, G.L., Probert, M.E., Robertson, M.J., Holzworth, D., Huth, N.I., Hargreaves, J.N., Meinke, H., Hochman, Z., 2003. Anoverview of APSIM, a model designed for farming systems simulation. Eur. J. Agron. 18, 267–288.

Kersebaum, K., 2007. Modelling nitrogen dynamics in soil-crop systems with HERMES. Nutr. Cycl. Agroecosyst. 77, 39–52.

Li, X., Zhu, C., Wang, J., Yu, J., 2012. Computer simulation in plant breeding. Adv. Agron. 116, 219–264.

Li, T., Hasegawa, T., Yin, X., Zhu, Y., et al., 2015. Uncertainties in predicting rice yield by current crop models under a wide range of climatic conditions. Global Change Biol. 21, 1328–1341.

Marcaida, M., Li, T., Angeles, O., Evangelista, G.K., Fontanilla, M.A., Xu, J., Gao, Y., Li, Z., Ali, J., 2014. Biomass accumulation and partitioning of newly developed Green Super Rice (GSR) cultivars under drought stress during the reproductive stage. Field Crops Res. 162, 30–38.

Martre, P., Jamieson, P.D., Semenov, M.A., Zyskowski, R.F., Porter, J.R., Triboi, E., 2006. Modelling protein content and composition in relation to crop nitrogen dynamics for wheat. Eur. J. Agron. 25, 138–154.

Martre, P., Semenov, M.A., Jamieson, P.D., 2007. Simulation analysis of physiological traits to improve yield, nitrogen use efficiency and grain protein concentration in wheat. In: Spiertz, J.H.J., Struik, P.C., Van Laar, H.H. (Eds.), Scale and Complexity in Plant Systems Research, Gene-Plant-Crop Relations. Springer, The Netherlands, pp. 181–201.

Martre, P., He, J., Gouis, J.L., Semenov, M.A., 2015a. In silico system analysis of physiological traits determining grain yield and protein concentration for wheat as influenced by climate and crop management. J. Exp. Bot. 66, 3581–3598.

Martre, P., Wallach, D., Asseng, S., Ewert, F., et al., 2015b. Multimodel ensembles of wheat growth: many models are better than one. Global Change Biol. 21, 911–925.

Metzger, M., Bunce, R., Jongman, R., Mücher, C., Watkins, J., 2005. A climatic stratification of the environment of Europe. Global Ecol. Biogeogr. 14, 549–563.

Mir, Affiliated withInternational Crops Research Institute for the Semi-Arid Tropics (ICRISAT)Division of Plant Breeding and Genetics, Sher-e-Kashmir University of Agricultural Sciences and Technology of Jammu (SKUAST-J) R.R., Zaman-Allah, M., Sreenivasulu, Affiliated withLeibniz Institute of Plant Genetics and Crop Plant Research (IPK) N., Trethowan, R., Varshney, Affiliated withInternational Crops Research Institute for the Semi-Arid Tropics (ICRISAT)CGIAR-Generation Challenge Programme (GCP), c/o CIMMYTSchool of Plant Biology (M084), Faculty of Natural and Agricultural Sciences, The University of Western Australia Email author R.K. 2012. Integrated genomics, physiology and breeding approaches forimproving drought tolerance in crops. Theor. App. Genet. 125, 625–645.

Miralles, D.J., Richards, R.A., 2000. Responses of leaf and tiller emergence and primordium initiation in wheat and barley to interchanged photoperiod. Ann. Bot. 85, 655–663.

Monfreda, C., Ramankutty, N., Foley, J.A., 2008. Farming the planet: 2. Geographic distribution of crop areas, and yields, physiological types, and net primary production in the year 2000. Global Biogeochem. Cycles 22, GB1022.

Moshelion, M., Halperin, O., Wallach, R., Oren, R., Way, D.A., 2015. Role of aquaporins in determining transpiration and photosynthesis in water-stressed plants: crop water-use efficiency growth and yield. Plant Cell Environ. 38, 1785–1793.

Nazarenko, L., Schmidt, G.A., Miller, R.L., Tausnev, N., et al., 2015. Future climate change under RCP emission scenarios with GISS ModelE2. J. Adv. Model. Earth Syst. 7, 244–267.

Nendel, C., Berg, M., Kersebaum, K.C., Mirschel, W., Specka, X., Wegehenkel, M., Wenkel, K.O., Wieland, R., 2011. The MONICA model Testing predictability for crop growth, soil moisture andnitrogen dynamics. Ecol. Model. 222, 1614–1625.

Palosuo, T., Kersebaum, K.C., Angulo, C., Hlavinka, P., et al., 2011. Simulation of winter wheat yield and its variability in different climates of Europe: a comparison of eight crop growth models. Eur. J. Agron. 35, 103–114.

Parry, M., Reynolds, M., Salvucci, M., Raines, C.A., Andralojc, P.J., Zhu, X.G., Price, G.D., Condon, A.G., Furbank, R.T., 2010. Raising yield potential of wheat: (II) increasing photosynthetic capacity and efficiency. J. Exp. Bot. 62, 453–467.

Peltonen-Sainio, P., Kangas, A., Salo, Y., Jauhiainen, L., 2007. Grain number dominates grain weight in cereal yield determination: evidence based on 30 years' multi-location trials. Field Crops Res. 100, 179–188.

Peltonen-Sainio, P., Muurinen, S., Rajala, A., Jauhiainen, L., 2008. Variation in harvest index of modern spring barley, oat and wheat under northern conditions. J. Agric. Sci. 146, 35–47.

Pirttioja, N., Carter, T.R., Fronzek, S., Bindi, M., et al., 2015. A crop model ensemble analysis of temperature and precipitation effects on wheat yield across a European transect using impact response surfaces. Clim. Res. 65, 87–105.

Porter, J.R., Xie, L., Challinor, A.J., Cochrane, K., Howden, S.M., Iqbal, M.M., Lobell, D.B., Travasso, M.I., 2014. Food security and food production systems. In: Climate Change 2014: Impacts, Adaptation, and Vulnerability. Part A: Global and Sectoral Aspects. Contribution of Working Group II to the Fifth Assessment Report of the Intergovernmental Panel on Climate Change. Cambridge University Press, Cambridge, United Kingdom and New York, NY, pp. 485–533.

Rötter, R.P., Palosuo, T., Pirttioja, N.K., Dubrovsky, M., Salo, T., Fronzek, S., Aikasalo, R., Trnka, M., Ristolainen, A., Carter, T.R., 2011a. What would happen to barley production in Finland if global warming exceeded 4 °C? A model-based assessment. Eur. J. Agron. 35, 205–214.

Rötter, R.P., Carter, T.R., Olesen, J.E., Porter, J.R., 2011b. Crop-climate models need an overhaul. Nat. Clim. Change 1, 175–177.

Rötter, R.P., Palosuo, T., Kersebaum, K.C., Angulo, C., Bindi, M., Ewert, F., Ferrise, R., Hlavinka, P., Moriondo, M., Olesen, J.E., Takáč, J., Trnka, M., 2012. Simulation of spring barley yield in different climatic zones of Northern and Central Europe: a comparison of nine crop growth models. Field Crops Res. 133, 23–36.

Rötter, R.P., Tao, F., Höhn, J.G., Palosuo, T., 2015. Use of crop simulation modelling to aid ideotype design of future cereal cultivars. J. Exp. Bot. 66, 3463–3476.

Rashid, H., Hirst, A., Dix, M., 2013. Atmospheric circulation features in the ACCESS model simulations for CMIP5: historical simulation and future projections. Aust. Meteorol. Oceanograph. J. 63, 145–160.

Ray, D.K., Ramankutty, N., Mueller, N.D., West, P.C., Foley, A., 2012. Recent patterns of crop yield growth and stagnation. Nat. Commun. 3, 1293.

Ray, D.K., Gerber, J.S., MacDonald, G.K., West, P.C., 2015. Climate variation explains a third of global crop yield variability. Nat. Commun. 6, 5989.

Reynolds, M.P., Quilligan, E., Aggarwal, P.K., et al., 2016. An integrated approach to maintaining cereal productivity under climate change. Global Food Secur. 8, 9–18.

Salo, T., Palosuo, T., Kersebaum, K.C., Nendel, C., Angulo, C., Ewert, F., Bindi, M., Calanca, T., Klein, T., Moriondo, M., Ferrise, R., Olesen, J.E., Patil, R.H., Ruget, F., Takác, J., Hlavinka, P., Trnka, M., Rötter, R.P., 2016. Comparing the performance of 11 crop simulation models in predicting yield response to nitrogen fertilisation. J. Agric. Sci. 154, 1218–1240.

Semenov, M.A., Stratonovitch, P., 2013. Designing high-yielding wheat ideotypes for a changing climate. Food Energy Secur. 2, 185–196.

Semenov, M.A., Stratonovitch, P., 2015. Adapting wheat ideotypes for climate change: accounting for uncertainties in CMIP5 climate projections. Clim. Res. 65, 123–139.

Shearman, V.J., Sylvester-Bradley, R., Scott, R.K., Foulkes, M.J., 2005. Physiological processes associated with wheat yield progress in the UK. Crop Sci. 45, 175–185.

Siddique, K.H.M., Tennant, D., Perry, M.W., Belford, R.K., 1990. Water use and water use efficiency of old and modern wheat cultivars in a Mediterranean-type environment. Aust. J. Agric. Res. 41, 431–447.

Stöckle, C., Donatelli, M., Nelson, R., 2003. CropSyst, a cropping systems simulation model. Eur. J. Agron. 18, 289–307.

Tao, F., Zhang, Z., 2010. Adaptation of maize production to climate change in North China Plain: quantify the relative contributions of adaptation options. Eur. J. Agron. 33, 103–116.

Tao, F., Zhang, Z., 2013. Climate change, wheat productivity and water use in the North China Plain: a new super-ensemble-based probabilistic projection. Agric. For. Meteorol. 170, 146–165.

Tao, F., Zhang, S., Zhang, Z., 2012. Spatiotemporal changes of wheat phenology in China under the effects of temperature, day length and cultivar thermal characteristics. Eur. J. Agron. 43, 201–212.

Tao, F., Zhang, S., Zhang, Z., Rötter, R.P., 2015. Temporal and spatial changes of maize yield potentials and yield gaps in the past three decades in China. Agric. Ecosyst. Environ. 208, 12–20.

Tebaldi, C., Knutti, R., 2007. The use of the multi-model ensemble in probabilistic climate projections. Philos. Trans. A: Math. Phys. Eng. Sci. 365, 2053–2075.

Tilman, D., Balzer, C., Hill, J., Befort, B.L., 2011. Global food demand and the sustainable intensification of agriculture. Proc. Natl. Acad. Sci. U. S. A. 108, 20260–20264.

USDA, 1999. Soil Taxonomy—A Basic System of Soil Classification for Making and Interpreting Soil Surveys. United States Department of Agriculture, Washington D.C., USA.

Wallach, D., Mearns, L.O., Ruane, A.C., et al., 2016. Lessons from climate modeling on the design and use of ensembles for crop modeling. Clim. Change, http://dx.doi.org/10.1007/s10584-016-1803-1 (in press).

Yin, X., Struik, P.C., Eeuwijk, F.A., van Stam, P., Tang, J., 2005. QTL analysis and QTL-based prediction of flowering phenology in recombinant inbred lines of barley. J. Exp. Bot. 56, 967–976.

Zilberman, D., 2015. IPCC AR5 overlooked the potential of unleashing agricultural biotechnology to combat climate change and poverty. Global Change Biol. 21, 501–503.

Table S1. Field experiments, crop management and climate characteristics for baseline and 2050s used in partially calibrating and validating crop models, and simulation experiments

Location	Jokioinen, Finland	Lleida, Spain
Latitude	60.81°N	41.63°N
Longitude	23.50°E	0.60°E
Environment	Boreal climate	Mediterranean climate
Average growing season	Middle of May to end of August	Middle of November to beginning of July
Soils		
Soil type	Vertic Cambisol	Xerofluvent typic
Soil depth	225cm	130cm
Permanent wilting point (m^3/m^3)	22%	16.7%
Field capacity (m^3/m^3)	40%	33.9%
Bulk density (g/cm^3)	1.5	1.4
Sand (%)	7.0%	39.0%
Clay (%)	11.8%	28.8%
Silt (%)	81.2%	32.3%
Crop management		
Cultivar	Annabelle	Hispanic

Sowing date (DOY)	13/05/2002 14/05/2009	08/11/1996 18/11/1997 16/11/1998
Total applied N fertilizer (kgN/ha)	90.0	Two N fertilization treatments: 0.0 and 120.0
Total irrigation (mm)	0.0	0.0
Phenology		
Heading (DOY)	01/07/2002 10/07/2009	18/04/1997 22/04/1998 10/05/1999
Maturity (DOY)	19/08/2002 21/08/2009	30/05/1997 05/06/1998 08/06/1999
Experimental year		
Mean growing season temperature	2002 (15.6) 2009 (14.0)	1997 (12.6) 1998 (11.9) 1999 (11.7)
Mean growing season precipitation	2002 (206.6) 2009 (200.7)	1997 (371.0) 1998 (191.9) 1999 (255.7)
Baseline		
Mean growing season	13.6	11.5

temperature (°C)		
Mean growing season precipitation (mm)	252.4	227.3
Climate change scenario		
GCM scenario examined	ACCESS, GISS and HadGEM	ACCESS, GISS and HadGEM
Mean growing season temperature (°C)	ACCESS (16.2), GISS (16.1) and HadGEM (17.0)	ACCESS (14.1), GISS (12.8) and HadGEM (13.9)
Mean growing season precipitation (mm)	ACCESS (284.0), GISS (266.3) and HadGEM (257.4)	ACCESS (185.8), GISS (225.9) and HadGEM (225.3)

Table S2. Crop models used in this study

Model (version)	Reference	Documentation
APSIM (V.7.7)	Keating et al., 2003	http://www.apsim.info/Wiki/
CropSyst (V 3.02)	Stockle et al., 2003	http://www.bsyse.wsu.edu/CS_Suite/CropSyst/index.html
HERMES (V4.26)	Kersebaum, 2007, 2011	http://www.zalf.de/en/forschung/institute/lsa/forschung/oekomod/hermes
MCWLA (V2.0)	Tao et al., 2009, 2013	Request from fulu.tao@luke.fi
MONICA (V1.2.5)	Nendel et al., 2011	http://monica.agrosystem-models.com
SIMPLACE<Lintul2, Slim>	Addiscott and Whitmore, 1991; Angulo et al., 2013	www.simplace.net/, http://models.pps.wur.nl/models
SiriusQuality (V2.0)	Martre et al., 2006; Ferrise et al., 2010	Request from pierre.martre@clermont.inra.fr
WOFOST (V7.1)	Boogaard et al., 1998	http://www.wofost.wur.nl

Table S3. Key genetic cultivar parameters in each crop model, the calibrated parameters values for baseline conditions, and the estimated parameters values ranges, for Jokioinen and Lleida, respectively.

Model	**Model parameters**	**Explainations of the parameters**	**Parameter value for Jokioinen**		**Parameter value for Lleida**	
			Value range	Calibrated value for baseline	Value range	Calibrated value for baseline
APSIM	photop_sens	Photoperiod response	2.0-5.0	3.5	2.0-5.0	3.5
	vern_sens	Vernalization response	0.5-1.5	1	0.5-1.5	1
	y_node_app_rate(2)	node phyllochron	67.5-82.5	75	90-110	100
	y_rue(3)	Radiation use efficiency for each phenological stage	1.116-1.364	1.24	1.116-1.364	1.24
	y_CO_2_te_modifier(2)	Factor of CO_2 effects in C3 crops	1.233-1.507	1.37	1.233-1.507	1.37
	transp_eff_cf(3)	Transpiration efficiency coefficient	0.00525-0.00675	0.006	0.00525-0.00675	0.006
	max_grain_size	Maximum grain size	0.085-0.115	0.1	0.05525-0.07475	0.065
	grains_per_gram_stem	Grains per gram of stem	28-36	32	21.875-28.125	25

CropSyst	GDD_Flw	Thermal time sowing to begin flowering (GDD, Tb= 0ºC)	700-800	750	1500-1700	1600
	GDD_Mty	Thermal time sowing to maturity (GDD, Tb= 0ºC)	1300-1400	1350	2100-2350	2270
	LAImax	Maximum LAI	4.0-6.0	5	5.0-7.0	6
	LWP_red	Leaf water potential that begins reduction of canopy expansion (J/kg)	-1000 to -1500	-1200	-1100 to -1700	-1200
	RUE	Radiation Use Efficiency (g/MJ)	2.3-3.0	2.8	2.3-3.0	2.56
	C_TB	Conversion coefficient transpiration / biomass (kPa·kg/m^3)	5.5-6.9	6.7	5.5-6.9	6.7
	MWU	Maximum water uptake (mm)	8.0-10	8.6	8.0-10	8.5
	HI	Harvest Index	0.40-0.60	0.53	0.3-0.5	0.42

	Tsum1	Temperature sum sowing to emergence	90-180	148	90-180	110
	Tsum3	Temperature sum double ridge to heading	250-600	575	250-600	285
	Tsum4	Temperature sum heading to flowering	130-180	130	130-180	145
	Tsum5	Temperature sum flowering to ripening	220-500	240	220-500	425
	DL	Daylength requirement until heading	16-20	20	16-20	17
HERMES	Amax	maximum CO_2 assimilation at light saturation (kg CO_2/ha leaf/h)	48-53	48	48-53	48
	Scr(5)	Critical threshold value for ratio of actual transpiration and potential transpiration to affect growth during grain filling	0.4-0.6	0.6	0.4-0.6	0.5

MCWLA	R_{maxvg2}	The maximum development rate (per day) from terminal spikelet initiation to flowering	0.018-0.058	0.038	0.007-0.037	0.022
	R_{maxrg}	The maximum development rate (per day) in the reproductive phases	0.022-0.062	0.042	0.023-0.053	0.038
	L_{AImax}	Maximum LAI (m^2m^{-2})	6.5-7.5	7	6.5-7.5	7
	L_{AIdg}	A parameter for LAI decreasing rate after flowering to maturity	0.3-0.7	0.5	0.3-0.7	0.5
	T_{Tmax}	Maximum transpiration rate (mm $m^{-2}day^{-1}$)	3.7387-7.7387	5.7387	3.7387-7.7387	5.7387
	α (Intrinsic quantum efficiency of CO_2 uptake)	Effective ecosystem-level quantum efficiency or Intrinsic quantum efficiency of CO_2 uptake in C3 plant	0.07-0.09	0.08	0.0757-0.0957	0.0857
	S_{cr}	Critical threshold value for ratio of transpiration and	0.4-0.6	0.4667	0.4-0.6	0.4667

		potential transpiration to affect growth				
	HI	Harvest index	0.44-0.64	0.54	0.14-0.34	0.24
MONICA	Tsum3	Temperature sum from double ridge to begin flowering	200–400	280	200–400	360
	Tsum5	Temperature sum during grain filling period	200–500	290	200–500	290
	LAI3	Specific leaf area (m^2kg dm leaf^{-1}) from double ridge to flowering	0.0010–0.0035	0.0019	0.0010–0.0035	0.0019
	Amax	Maximum assimilation rate	25–55	30	25–55	30
	kc3	kc factor from double ridge to flowering	0.5–1.4	1	0.5–1.4	1
	kc5	kc factor during grain filling period	0.5–1.4	0.8	0.5–1.4	0.8
	Scr3	Critical threshold value for ratio of transpiration and	0.3–1.0	0.8	0.3–1.0	0.8

		potential transpiration to affect growth, from double ridge to flowering				
	Scr5	Critical threshold value for ratio of transpiration and potential transpiration to affect growth, during grain filling period	0.3–1.0	0.6	0.3–1.0	0.6
SIMPLACE	AirTemperatureSumAnthesis	Pre-anthesis degree days	600-1100	861.5	1000-1400	1221
	AirTemperatureSumMaturity	Maturity degree days	1200-1600	1440	1500-1850	1677
	RGRL	Relative growth rate of LAI during exponential growth (RGRL)	0.015-0.025	0.02	0.002-0.006	0.004
	SLA	Specific leaf area [cm^2/g]	0.02-0.035	0.026	0.02-0.035	0.023
	LUE	Light use efficiency of PAR [g/MJ]	3.0-3.4	3.2	2.7-3.1	2.9
	M2H	Factor accounting for average time between	0 - 0.3	0.1	1.1 - 1.5	1.3195

		maturity and harvest				
	StartWaterSensitiveDVS	Development stage when sensitive phase to drought stress starts	0.5 - 1.2	0.85	0.5 - 1.2	1
SiriusQuality	P	Phyllochron (°Cday/leaf)	110 - 150	135	110 - 150	135
	Dgf	Grain filling duration (from anthesis to physiological maturity (°Cday)	350 - 550	450	300 - 500	335
	AreaPL	Maximum potential surface area of the penultimate leaf lamina (cm²/lamina)	20 - 40	30	20 - 40	30
	NLL	Number of leaves produced after floral initiation (leaf)	4 - 6	5	4 - 6	5
	LUEDiffuse	Potential radiation use efficiency under overcast conditions (g(DM)/MJ (PAR))	2.3 - 4.8	4.5	2.3 - 4.8	3.8
	MaxDSF	Maximum rate of	2.5-5	4	2.5-5	4

		acceleration of leaf senescence in response to soil water deficit (dimensionless)				
	UpperFTSWgs	Fraction of transpirable soil water threshold for which the stomatal conductance starts to decrease (dimensionless)	0.4 - 0.6	0.5	0.4 - 0.6	0.5
	BetaRWU	Efficiency of the root system to extract water through the vertical soil profile (dimensionless)	0.05 - 0.10	0.07	0.05 - 0.10	0.07
	TSUM1	Pre-anthesis degree days	600-850	720	1350-1500	1480
	TSUM2	Post-anthesis degree days	600-700	640	650-800	750
	RGRLAI	Relative initial leaf growth rate	0.003-0.0055	0.008	0.003-0.012	0.00375
	SLATB	Specific leaf area (SLA) as	0.0022-0.0055	0.0035	0.0022-0.0055	0.0025

WOFOST		function of DVS				
	A_{max}	Maximum leaf assimilation rate [kg ha-1 hr-1]at DVS 0 to 1.2	32-38	35	32-42	37.5
	RRI	maximum daily increase in rooting depth [cm d^{-1}]	0.5-4.0	2	0.5-4.0	1.5
	RDMCR	maximum rooting depth [cm]	50-150	80	50-150	125
	FOTB	Partitioning fraction for storage organs at DVS 1.01	0.8-0.99	0.85	0.8-0.99	0.85